Results

The studied 100 cases of prostate cancer were obtained by needle biopsy (34 cases), TURP chips (29 cases) and prostatectomy (37 cases) specimens.

Age distribution of examined prostate cancer cases:

The mean patient age was 66.7 years (ranged from 42 to 90 years) and the median was 66.5 years.The age distribution was shown in Table (3) and Graph (1).

Table (3):Age distribution of 100 prostate carcinoma cases:

Age groups (decades)	Total no.	Percentage(%)
41-50	2	2%
51-60	23	23%
61-70	40	40%
71-80	31	31%
81-90	4	4%

The peak age incidence in prostate carcinoma was from 61-70 years .

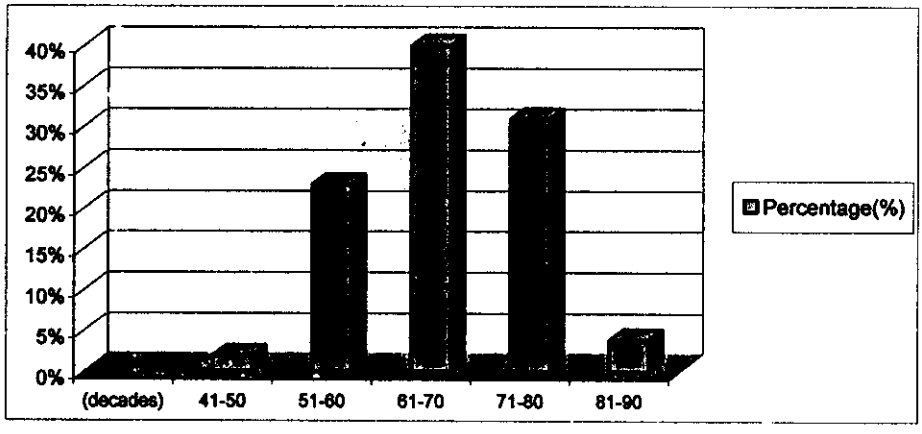

Graph(1):Age distribution of prostate cancers examined.

I. Histopathologic features:

All studied prostate cancer cases (100%) were acinar adenocarcinomas of the peripheral zone.

The incidence of high-grade PIN:

a) In all prostate cancer cases:

High- grade PIN was detected in 25 out of 100 cases (25%) of prostate cancer examined, of which 14 cases (56%) were of tufting pattern (Fig.10), 5 (20%) of papillary pattern (Fig.11), 4 (16%) of cribriforming pattern (Fig.12), and 2 (8%) of flat pattern (Fig.13).

b) In different prostate specimens:

In prostatectomies: high- grade PIN was detected in 15 out of 37 cases (40.5 %).

In TURP chips: high- grade PIN was detected in 6 out of 29 cases (20.7%).

In needle biopsies: high- grade PIN was detected in 4 out of 34 cases (11.8%).

Histopathologic patterns of prostatic carcinoma:

According to ***Bostwick (1994),*** histopathologic patterns were as follows *(Table 4)*:

Pattern 2: included 15 cases with well-differentiated glands pattern (Fig.14) with associated perineural invasion in 4 cases and vascular embolization in 3 cases.

Pattern 3: included 42 cases, of which 36 cases were of pattern 3 glands (with infiltrative appearance among larger benign glands), 3 of cribriforming pattern, and 2 cases with papillary pattern.

Of the 36 cases with pattern 3 glands (Fig.15), one case was associated with bilharzial changes. Multifocality could be detected in only one case which also showed high-grade PIN. Perineural invasion was detected in 8 cases of them and vascular embolization in 11 cases.

Of the 3 cases with cribriforming pattern (Fig.12), 2 cases was associated with bilharzial changes and one case with associated perineural invasion.

Of the 2 cases with papillary pattern (Fig.16),one case was associated with bilharzial changes.

Pattern 4: included 29 cases , of which 28 cases were of fused glands pattern (Fig.17) (with raggedly infiltrating edges and poor acinar formation, and with some cords and chains of malignant epithelial cells), and one case of clear cell carcinoma pattern (Fig.18).

Of the 28 cases with fused glands pattern, one case showed neuroendocrine differentiation, 2 cases with focal comedo necrosis (Fig.19), 2 cases with associated bilharzial changes,and one case with associated dysplastic urothelial changes. Multifocality could be detected in only one case which also showed high-grade PIN. Perineural invasion was detected in 8 cases of them and vascular embolization in 7 cases.

Pattern 5: included 14 cases, of which 12 were of anaplastic pattern (Fig.20) (being disposed in sheets and solid groups ,or individually infiltrating cells of poorly differentiated type, with difficulty to identify gland lumina),and 2 of mucoid carcinoma pattern (Fig.21).

Of the 12 cases with anaplastic pattern, one case showed neuroendocrine differentiation (Fig.22), and another case with focal clear cell pattern.

Perineural invasion was detected in 7 cases of them and vascular embolization in 2 cases.

Of the 2 cases with mucoid carcinoma pattern, one case was associated with dysplastic urothelial changes, supporting "the field effect" theory.

Table(4):Distribution of histopathologic patterns in examined prostate cancer cases:

Histopathologic pattern	Number of cases	Percentage
Pattern 2	*15*	*15%*
Pattern 3	*42*	*42%*
Pattern 4	*29*	*29%*
Pattern 5	*14*	*14%*
Total	**100**	**100%**

Nuclear Grading:

Out of studied 100 prostate cancer cases, 13 cases were of Grade I (13%), 63 of Grade II (63%) and 24 of Grade III (24%) *(Table,5; Graph, 2).*

Table (3):Distribution of nuclear grade in studied cases with prostate cancer:

Nuclear grade	*Number of cases*	*Percentage*
G1	*13*	*13%*
G2	*63*	*63%*
G3	*24*	*24%*
Total	*100*	*100%*

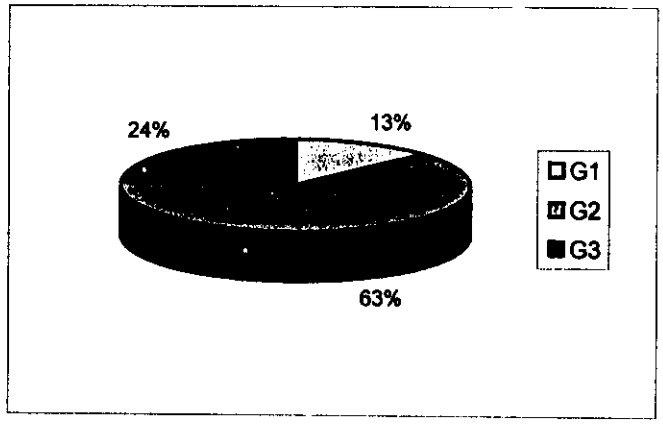

Graph(2):Distribution of nuclear grade in examined cases with prostate cancer.

Gleason Sum Score:

Out of the 100 cases examined, one case was of G.S.2, 3 were of G.S.3, 5 of G.S.4, 10 of G.S.5, 33 of G.S.6, 24 of G.S.7, 12 of G.S.8, 11 of G.S.9, and one was of G.S.10 *(Table, 6)*.

Table(6): Distribution of Gleason Sum Score in studied cases with prostate cancer:

Gleason Sum Score	Number of cases	Percentage
G.S.2	1	1%
G.S.3	3	3%
G.S.4	5	5%
G.S.5	10	10%
G.S.6	33	33%
G.S.7	24	24%
G.S.8	12	12%
G.S.9	11	11%
G.S.10	1	1%
Total	100	100%

According to the cutoff value which is G.S.S.7.

The distribution of Gleason Sum Score in prostate cancer cases was shown in *(Table 7,Graph 3)*:

Fifty two out of 100 (52%) prostate cancer cases were of low-grade tumours (G.S.<7) and 48 (48%) were of high-grade (G.S. ≥ 7).

Table (5):Distribution of Gleason Sum Score in studied cases of prostate cancer:

Gleason Sum Score	*Number of cases*	*Percentage*
G.S.S.<7	*52*	*52%*
G.S.S. ≥7	*48*	*52%*
Total	*100*	*100%*

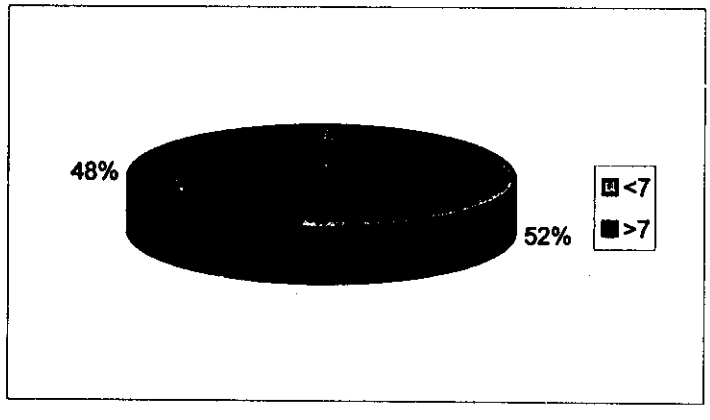

Graph(3):Distribution of Gleason Sum Score in examined cases with prostate cancer.

Pathologic Staging:

TNM pathologic staging could be accessible only in 37 prostatectomy specimens ; of which 18 cases (48.7%) were of pathologic stage 2 (pT2), 12(32.4%) of pathologic stage 3 (pT3), and 7(18.9%) of pathologic stage 4 (pT4) with lymph node metastases. Twenty-two out of 37 (59.5%) prostatectomy cases showed perineural invasion (Fig.23), 19 cases (51.5%) showed vascular embolization (Fig.24), and 18 cases (48.6%) showed capsular penetration (Fig.25).

The distribution of pathologic staging in prostatectomy cases was shown in*Table 8* and *Graph 4.*

Table (6):Distribution of pathologic stage in studied prostatectomy cases with prostate cancer:

Pathologic stage	*Number of cases*	*Percentage*
pT-1	-	-
pT-2	*18*	*48.7%*
pT-3	*12*	*32.4%*
pT-4	*7*	*18.9%*
Total	*37*	*100%*

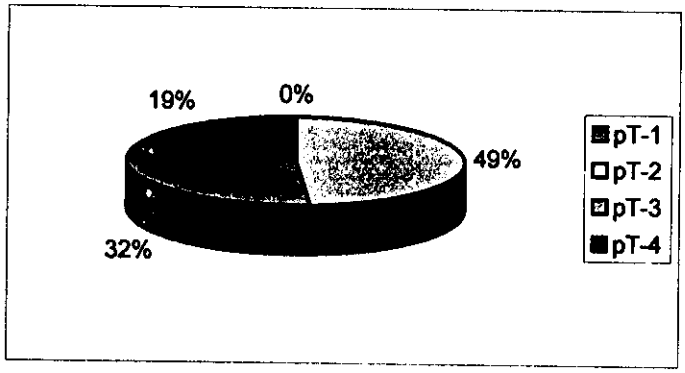

Graph(4):Distribution of pathologic stage in examined prostatectomy cases with prostate cancer.

Correlation between histopathologic pattern and nuclear grade in all cases examined:

All the 15 cases (100%) with pattern 2 were of low-nuclear grade (G1, G2).

Out of the 42 cases with pattern 3, 40 cases(95.2%) were of low-nuclear grade (G1, G2) and 2 (4.8%) of high-nuclear grade (G3).

Out of the 29 cases with pattern 4, 16 cases(55.2%) were of low-nuclear grade (G1, G2) and 13 (44.8%) of high-nuclear grade (G3).

Out of the 14 cases with pattern 5, 5 cases(35.7%) were of low-nuclear grade (G1, G2) and 9 (64.3%) of high-nuclear grade (G3).

This means; the worse the histopathologic pattern, the higher the nuclear grade*(Table,9)*.

A high statistically significant correlation between histopathologic pattern and nuclear grade was found *($P<0.01$)*.

Correlation between histopathologic pattern and Gleason Sum Score in all cases examined:

Out of the 15 cases with pattern 2, 13 cases(86.7%) were of low-G.S.S. and 2 (13.3%) of high- G.S.S.

Out of the 42 cases with pattern 3, 35 cases(83.3%) were of low-G.S.S. and 7 (16.7%) of high- G.S.S.

Out of the 29 cases with pattern 4, 3 cases(10.3%) were of low-G.S.S. and 26 (89.7%) of high- G.S.S.

Out of the 14 cases with pattern 5, one case (7.1%) was of low-G.S.S. and 13 (92.9%) were of high- G.S.S.

This means; the worse the histopathologic pattern, the higher the Gleason Sum Score *(Table,9)*.

A high statistically significant correlation between histopathologic pattern and Gleason Sum Score was found *(P<0.01)*.

Table (9):Correlation between histopathologic patterns and that of nuclear grade and Gleason Sum Score:

Histopathologic pattern	Nuclear grade			G.S.S.	
	G1	G2	G3	<7	>7
Pattern 2	9(60%)	6(40%)	-	13(86.7%)	2(13.3%)
Pattern 3	4(9.5%)	36(85.7%)	2(4.8%)	35(83.3%)	7(16.7%)
Pattern 4	-	16(55.2%)	13(44.8%)	3(10.3%)	26(89.7%)
Pattern 5	-	5(35.7%)	9(64.3%)	1(7.1%)	13(92.9%)
Total	13	63	24	52	48

Correlation between nuclear grade and G. S. Score in all cases:

Out of the 76 low-nuclear grade tumours (G1,G2), 52 cases (68.4%) were of low-Gleason Sum Score and 24 (31.6%) were of high-Gleason Sum Score .

All the 24 cases with high-nuclear grade (G3) were of high-Gleason Sum Score.

So, nuclear grade is directly proportionate to G.S.S.

Statistically,a significant high positive correlation between G.S.S. and nuclear grade was found ($p<0.01$) *(Table,10;Graph,5)*.

Table (10):Correlation between nuclear grade and Gleason Sum Score in all cases:

Nuclear grade	GSS		Total
	<7	≥ 7	
G1	13(100%)	-	13
G2	39(61.9%)	24(38.1%)	63
G3	-	24(100%)	24
Total	52	48	100

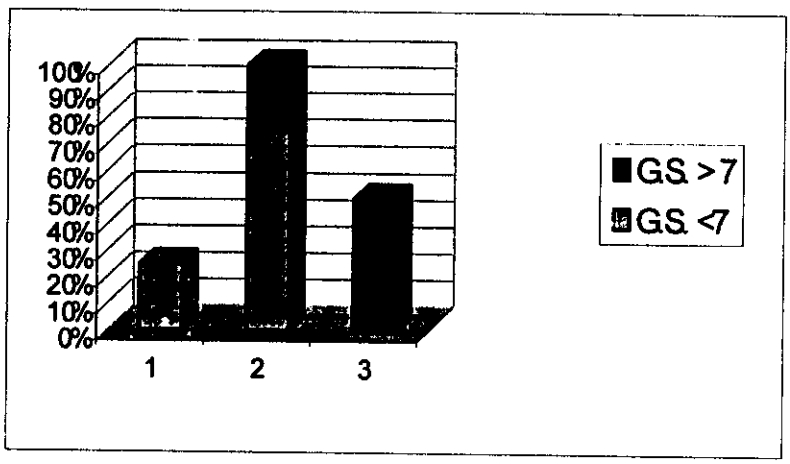

Graph(5): G.S.Score in relation to nuclear grade in all cases.

Correlation between nuclear grade and pathologic stage in prostatectomy specimens:

In prostatectomy specimens, 17 out of 31(54.8%) low-nuclear grade tumours(G1,G2)were of pT-2 tumours , 10 (32.3%) were of pT-3 tumours and 4 (12.9%) were of pT-4 tumours .

Out of the 6 high- nuclear grade tumours(G3), one case (16.7%) was of a pT-2 tumour, 2 (33.3%) of pT-3 and 3 (50%) of pT-4 tumours.

So, the higher the nuclear grade, the more advanced the pathologic stage. There was a high statistically significant positive correlation between pathologic stage and nuclear grade ($P<0.01$) *(Table,11;Graph,6)*.

Table (11):Correlation between nuclear grade and pathologic stage in prostatectomy specimens:

Nuclear Grade	pT-stage			Total
	pT-2	pT-3	pT-4	
G1	4(100%)	-	-	4
G2	13(48.2%)	10(37%)	4(14.8%)	27
G3	1(16.7%)	2(33.3%)	3(50%)	6
Total	18	12	7	37

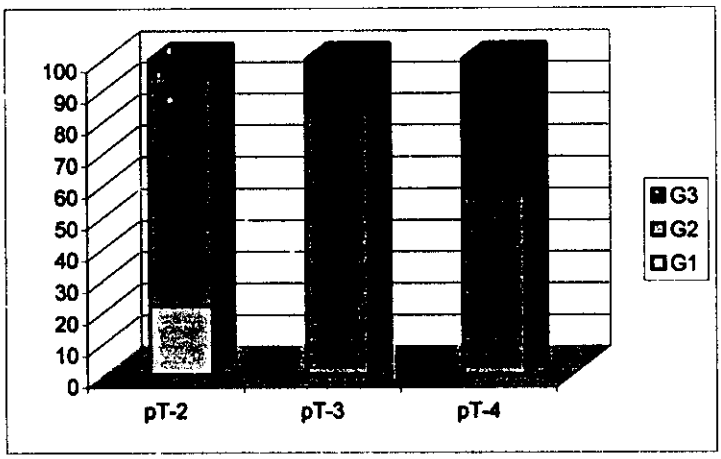

Graph(6): Pathologic stage in relation to nuclear grade in prostatectomy specimens.

Correlation between Gleason Sum Score and pathologic stage in prostatectomy specimens:

In prostatectomy specimens, 17 out of 18 cases (94.4%) of pT-2 were of low-Gleason Sum Score and one (5.6%) was of a high-Gleason Sum Score.

Seven out of the 12 cases of pT-3 (58.3%) were of low-Gleason Sum Score and 5 (41.7%) were of high-Gleason Sum Score.

Two out of the 7 cases of pT-4 tumours (28.6%) were of low-Gleason Sum Score and 5 (71.4%) were of high-Gleason Sum Score.
So, the higher the G.S.S., the more advanced the pathologic stage. There was a highly statistically significant positive correlation between G.S.S. and pathologic stage ($p<0.01$) *(Table,12;Graph,7)*.

Table (12):Correlation between Gleason Sum Score and pathologic stage in prostatectomy specimens:

G.S.S	pT-stage			Total
	PT-2	PT-3	PT-4	
<7	17(94.4%)	7(58.3%)	2(28.6%)	26
≥ 7	1(5.6%)	5(41.7%)	5(71.4%)	11
Total	18	12	7	37

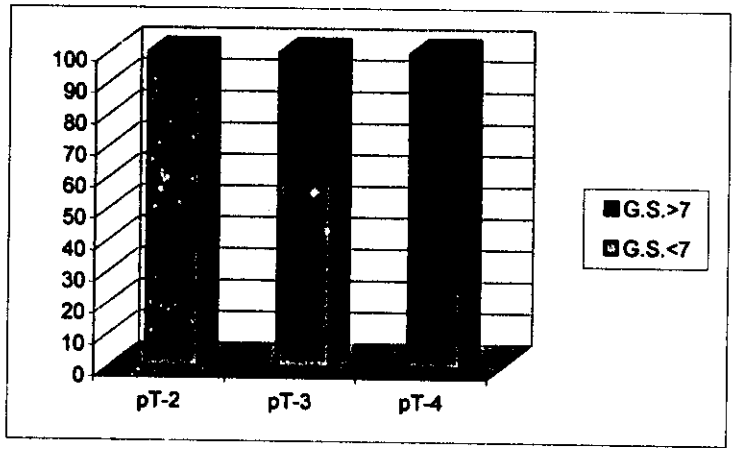

Graph(7):Pathologic stage in relation to G.S.Score in prostatectomy specimens.

II. Immunohistochemical Staining Results:

1) CD44 Results:

*** In the control cases:**

No immunolabeling was found in any of the negative controls. Intense immunostaining of the stratified squamous epithelium of the skin used as a positive control tissue (Fig. 26). Internal positive controls (benign glands and lymphocytes) were present in almost all radical prostatectomies and TURP specimens. In normal prostate tissue, CD44s labelling of basal cells was always observed, whereas normal epithelial secretory cells were not labelled.

*** CD44 expression in 100 cases of prostatic carcinoma:**

Sixteen cases (16%) showed absent CD44 expression , 26 (26%) showed CD44 expression less than 10%, 23(23%)showed CD44 positive immunostaining in 10-25 % of the tumour cells, 13 (13%) showed CD44 positive immunostaining in 25-50 % of the tumour cells, and 22 (22%) showed CD44 expression >50% *(Table 13;Graph 8)*.

According to the method of validation, the cutoff value was of CD44 expression <10%.

Among the 100 cases of prostate cancer examined, 42 cases showed absent or <10% CD44 expression and 58 cases showed >10% CD44 expression *(Table 14)*.

Table(13):Distribution of CD44 expression in the examined prostate carcinoma cases:

CD44 expression	*Number of cases*	*Percentage*
absent	*16*	*16%*
<10%	*26*	*26%*
10-25%	*23*	*23%*
25-50%	*13*	*13%*
>50%	*22*	*22%*
Total	*100*	*100%*

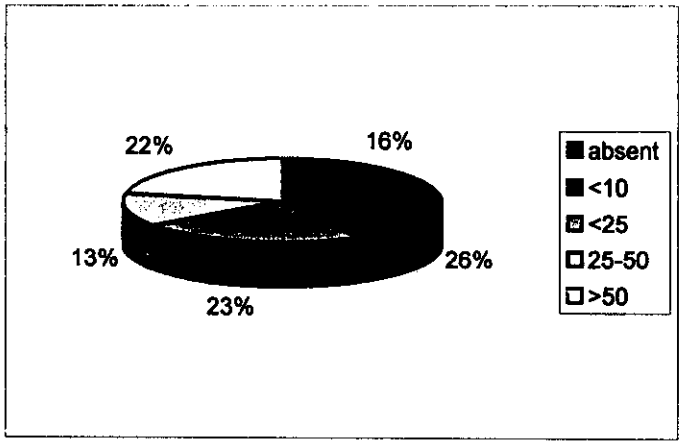

Graph(8): Distribution of CD44 expression in examined prostate cancer cases.

Table(14): CD44 expression in the examined prostate carcinoma cases:

CD44 expression	*Number of cases*	*Percentage*
<10%	*42*	*42%*
>10%	*58*	*58%*
Total	*100*	*100%*

Correlation between histopathologic pattern and CD44 expression :

Out of the 15 cases with pattern 2 , 5 cases(33.3%) showed CD44 expression <10% and 10 (66.7%) showed CD44 expression >10%.

Out of the 42 cases with pattern 3, 12 cases(28.6%) showed CD44 expression <10% and 30 (71.4%) showed CD44 expression >10%.

Out of the 29 cases with pattern 4, 20 cases(69%) showed CD44 expression <10% and 9 (31%) showed CD44 expression >10%.

Out of the 14 cases with pattern 5, 5 cases (35.7%) showed CD44 expression <10% and 9 (64.3%) showed CD44 expression >10%.

This means; the worse the histopathologic pattern, the more the reduction of CD44 expression *(Table,15)*. Although this correlation was statistically insignificant *(P>0.01)*.

Table(15):Correlation between CD44 expression and pathologic patterns:

Histopathologic pattern	CD44 expression		Total
	<10%	>10%	
Pattern 2	5(33.3%)	10(66.7%)	15
Pattern 3	12(28.6%)	30(71.4%)	42
Pattern 4	20(69%)	9(31%)	29
Pattern 5	5(35.7%)	9(64.3%)	14
Total	42	58	100

Correlation between CD44 expression and nuclear grade in all cases:

Twenty six out of 76 (34.2 %) low-nuclear grade tumours (G1,2) showed CD44 expression < 10 % and 50 (65.8%) showed CD44 expression > 10 % (Fig. 27). While, 16 out of 24 (66.6%) high-nuclear grade tumours (G3) showed CD44 expression <10 % and 8 (33.3%) showed CD44 expression > 10 % *(Table,16;Graph,9)*.

Thus, the higher the nuclear grade, the more reduction of CD44 expression. A statistically significant inverse correlation between nuclear grade and CD44 expression was found ($P < 0.05$).

Table (16):CD44 expression according to nuclear grade in all cases:

Nuclear grade	CD44 Expression		Total
	< 10 %	> 10 %	
G1	4(30.8%)	9(69.2%)	13
G2	22(34.9%)	41(65.1%)	63
G3	16(66.7%)	8(33.3%)	24
Total	42	58	100

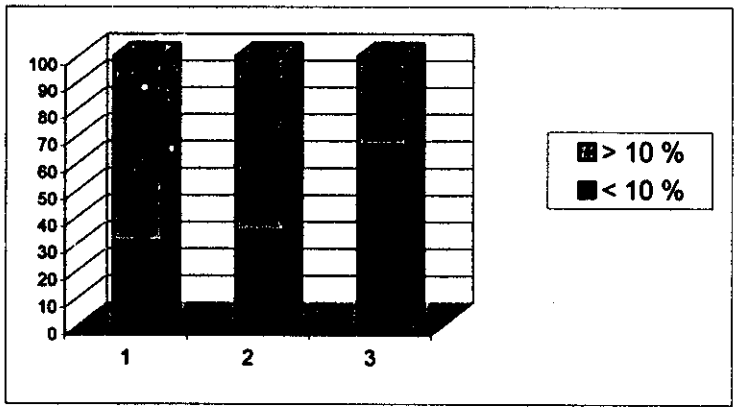

Graph(9):CD44 expression in relation to nuclear grade in all cases.

Correlation between CD44 expression and Gleason Sum Score in all cases:

Of the 52 prostate cancer cases with low- Gleason Sum Score (G.S. <7), 13 cases (25%) showed CD44 expression < 10% and 39 (75%) showed CD44 expression > 10% (Fig. 28). While of the 48 cases with high- Gleason Sum Score (G.S. ≥7), 29 cases (60.4%) showed CD44 expression < 10% (Fig. 29, 30) and 19 cases (39.6%) showed CD44 expression >10 *(Table,17; Graph,10)*.

So, decreased CD44 expression with evolution into high-grade tumours was noted. There was a high statistically significant inverse correlation between CD44 expression and G.S.Score(P<0.01).

Table (17): CD44 expression according to *Gleason Sum Score* in all cases:

G.S.S.	CD44 Expression		Total
	< 10 %	> 10 %	
< 7	13(25%)	39(75%)	52
≥ 7	29(60.4%)	19(39.6%)	48
Total	42	58	100

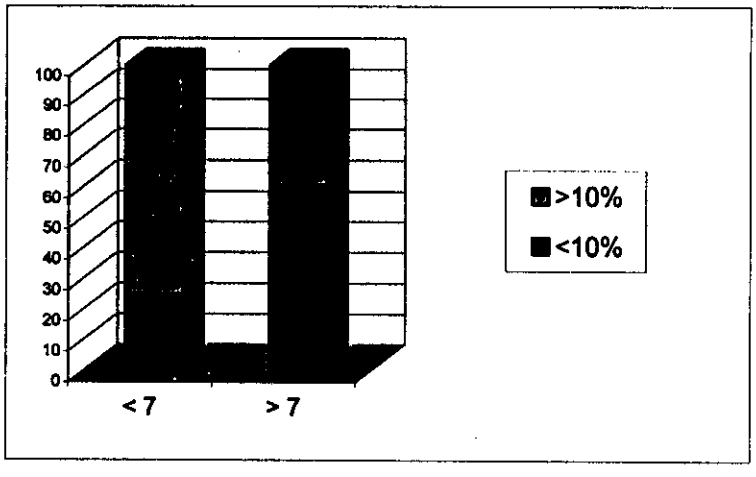

Graph(10):CD44 expression in relation to G.S.Score in all cases.

Correlation between CD44 expression and pathologic stage in prostatectomy specimens:

Out of the 14 cases that showed CD44 expression <10 %, 4 cases (28.6%) were of pT2 , 4 (28.6%) of pT3 and 6 (42.8%) of pT-4 tumours *(Table,18; Graph,11)*.

While, 14 out of 23 cases (60.9%) with CD44 expression > 10% were of pT2, 8 (34.8%) of pT3 and one case (4.3%) was of a pT-4 tumour.

So, there was reduced CD44 expression with evolution into advanced stages. Statistically, there was a high significant inverse correlation between the pathologic stage of prostate cancer and the CD44 expression ($p<0.01$).

Table (18): Pathologic stage in relation to CD44 expression results in prostatectomy specimens:

pT – stage	CD44 expression		Total
	< 10 %	> 10 %	
pT-2	4(28.6%)	14(60.9%)	18
pT-3	4(28.6%)	8(34.8%)	12
pT-4	6(42.8%)	1(4.3%)	7
Total	14	23	37

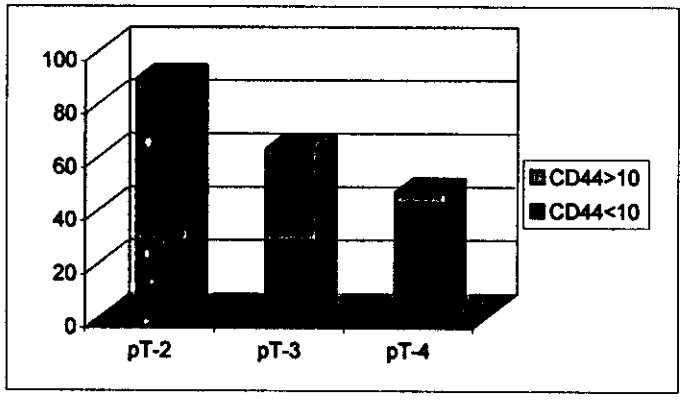

Graph(11):CD44 expression in relation to pathologic stage in prostatectomy specimens.

CD44 expression in relation to lymph node status in 37 prostatectomy specimens examined:

In prostatectomy specimens, there were 7 node-positive cases, of which 6 cases (85.7%) showed CD44 expression <10% [2 cases (33.3%) of them were negative for CD44 expression] and only one case (14.3%) showed CD44 expression >10% which was of a low-G.S.Score tumour. While, in the 30 node-negative cases, 8 cases (26.7%) showed CD44 expression <10% and 22 (73.3%) showed CD44 expression >10% *(Table 19;Graph 12)*.

There was a highly statistically significant inverse correlation between CD44 expression and lymph node status ($p<0.01$).

Table (19): CD44 expression in relation to lymph node status in prostatectomy specimens:

Patient group	CD44 expression		Total
	< 10 %	> 10 %	
Node-negative cases	8(26.7%)	22(73.3%)	30
Node-positive cases	6(85.7%)	1(14.3%)	7
Total	14	23	37

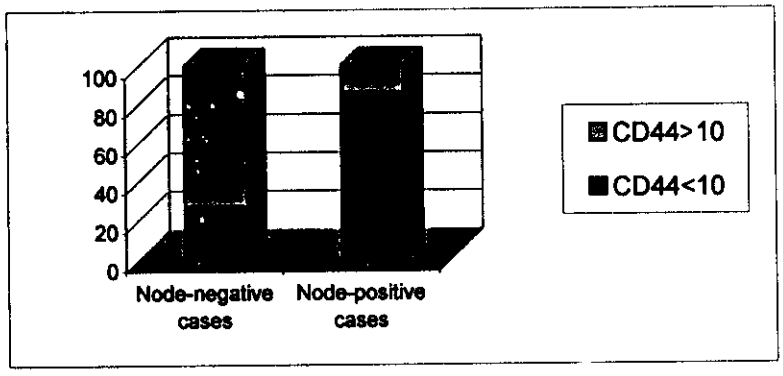

Graph(12): CD44 expression in relation to lymph node status in prostatectomy specimens.

2) MIB-1 Results:

No immunolabeling was found in any of the negative controls. Intense immunostaining of the lymphocytes in lymph follicles of the tonsil used as a positive control tissue (Fig. 31).

In BPH and in adenosis, MIB-1 positive nuclear immunostaining cells were of basal origin, although some luminal cells were also found to be MIB-1 positive in adenosis.

In PIN, a marked shift from the basal to the luminal compartment was noted, particularly in high- grade PIN.

MIB-1 expression in studied cases of prostatic carcinoma:

Fifty five cases (55%) showed positive immunostaining of tumour cell nuclei for MIB-1 *(Table 20)* .

The range of MIB-1 positive tumour cells was 1% to 75%, with a median of 15%.

By the validation method, 27 out of 100 cases showed MIB-1 expression > 15%, and 73 cases showed MIB-1 expression < 15% , of which 45 cases (61.6%) were negative for MIB-1 expression and 28 (38.4%) showed positive immunostaining for MIB-1 < 15% *(Table 20)*.

Table(20)Distribution of MIB-1 expression in examined prostate cancer cases::

MIB-1 expression	*No. of cases*	*Percentage*
Negative	*45*	*45%*
<10%	*17*	*17%*
10-15%	*11*	*11%*
15-25%	*10*	*10%*
25-50%	*9*	*9%*
>50%	*8*	*8%*
Total	*100*	*100%*

Correlation between histopathologic pattern and MIB-1 expression :

Out of the 15 cases with pattern 2 , 10 cases(66.7%) showed MIB-1 expression <15% and 5(33.3%) showed MIB-1 expression >15%.

Out of the 42 cases with pattern 3, 33 cases(78.6%) showed MIB-1 expression <15% and 9 (21.4%) showed MIB-1 expression >15% (Fig. 32).

Out of the 29 cases with pattern 4, 21 cases(72.4%) showed MIB-1 expression <15% and 8 (27.6%) showed MIB-1 expression >15% (Fig. 33).

Out of the 14 cases with pattern 5, 9 cases (64.3%) showed MIB-1 expression <15% and 5 (35.7%) showed MIB-1 expression >15%.

This means; the worse the histopathologic pattern, the more the proliferative activity of the tumour *(Table,21)*. However, this correlation was statistically insignificant *(P>0.01)*.

Table(21):Correlation between MIB-1 expression and pathologic patterns:

Histopathologic pattern	MIB-1 expression		Total
	<15%	>15%	
Pattern 2	10(66.7%)	5(33.3%)	15
Pattern 3	33(78.6%)	9(21.4%)	42
Pattern 4	21(72.4%)	8(27.6%)	29
Pattern 5	9(64.3%)	5(35.7%)	14
Total	73	27	100

MIB-1 expression in relation to nuclear Grade in all cases:

Twenty out of 76 (26.3%) low –nuclear grade tumours (G1,2) showed MIB-1 expression >15% and the remaining 56 cases (73.7%) showed MIB-1 expression <15% *(Table 22;Graph13)*.

Seven out of 24 (29.2%) high-nuclear grade tumours (G3) showed MIB-1 expression>15% (Fig. 34) and the remaining 17 cases (70.8%) showed MIB-1 expression <15%

It was found that; the higher the nuclear grade , the more the proliferative activity of the tumour , but statistically this correlation was insignificant *(P>0.01)*.

Table (22): MIB-1 expression according to nuclear grade in all cases:

Nuclear grade	MIB-1 Expression		Total
	< 15 %	> 15 %	
1	11(84.6%)	2(15.4%)	13
2	45(71.4%)	18(28.6%)	63
3	17(70.8%)	7(29.2%)	24
Total	73	27	100

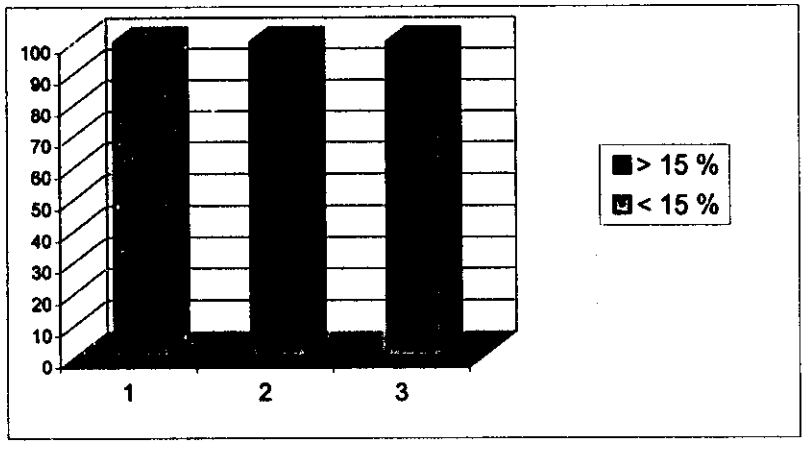

Graph(13):MIB-1 expression in relation to nuclear grade in all cases.

Correlation between MIB-1 expression and Gleason Sum Score in all cases:

Ten out of 52 (19.2%) low-Gleason Sum Score tumours showed MIB-1 expression >15% and 42 (80.8%) showed MIB-1 expression <15% (Fig. 36, 37). While, 17 out of 48 (35.4%) high- Gleason Sum Score tumours showed MIB-1 expression > 15% (Fig. 35) and 31 (64.6%) showed MIB-1 expression <15% *(Table 23;Graph 14)*.

So, the higher the grade , the greater the MIB-1 expression .

There was a direct correlation between the Gleason Sum Score and the proliferative activity of the tumour , although it was statistically insignificant *(p>0.01)*.

Table (23): MIB-1 expression according to Gleason Sum Score in all cases:

MIB-1 Expression	Gleason Sum Score		Total
	<7	≥7	
<15%	42(80.8%)	31(64.6%)	73
>15%	10(19.2%)	17(35.4%)	27
Total	52	48	100

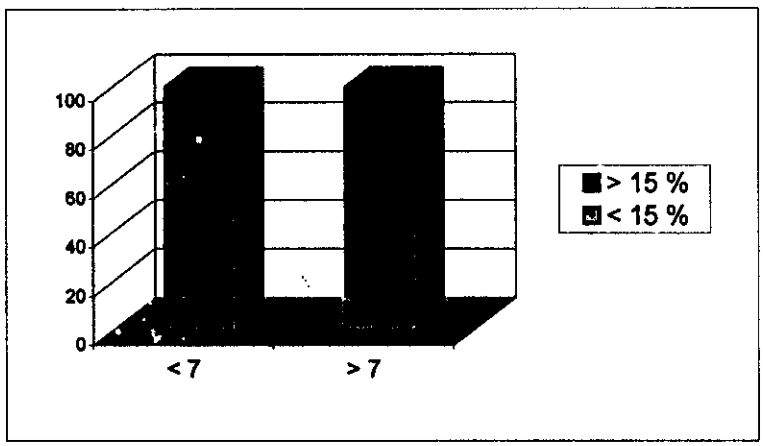

Graph(14):MIB-1 expression in relation to G.S.Score in all cases.

Correlation between MIB-1 expression and pathologic stage in prostatectomy specimens:

Of the 14 cases that showed MIB-1 expression >15% ,4 cases (28.6%) were of pT 2 , 5 (35.7%) of pT3 and 5 (35.7%) of pT-4.

Of the 23 cases that showed MIB-1 expression < 15%, 14 cases (60.9%) were of pT2 , 7 (30.4%) of pT3 and 2 (8.7%) of pT4 *(Table,24 ; Graph,15)*.

So, increased MIB-1 expression with evolution into advanced stages was noted. Statistically, a significant direct positive relation between the pathologic stage in prostatectomy specimens and the proliferative activity of the tumour was found ($p<0.05$).

Table (24): Distribution of Pathologic stage in relation to MIB-1 expression in prostatectomy specimens:

pT – stage	MIB-1 expression		Total
	< 15 %	> 15%	
pT-2	14(60.9%)	4(28.6%)	18
pT-3	7(30.4%)	5(35.7%)	12
pT-4	2(8.7%)	5(35.7%)	7
Total	23	14	37

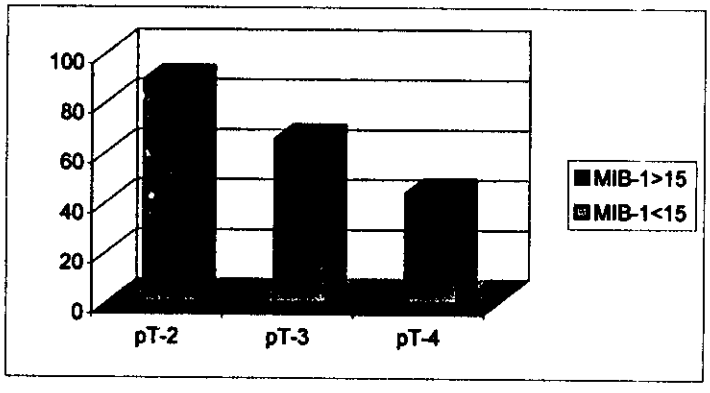

Graph(15):MIB-1 expression in relation to pathologic stage in prostatectomy specimens.

MIB-1 expression in relation to lymph node status in prostatectomy specimens :

In prostatectomy specimens, 2 (28.6%) out of the 7 node-positive cases showed MIB-1 expression <15% (both were negative for MIB-1 expression) and 5 cases (71.4%) showed MIB-1 expression >15% ,while in the 30 node-negative cases, 21 cases(70%)showed MIB-1 expression <15% and 9 (30%) showed MIB-1 expression >15% *(Table 25; Graph 16)* .

So, increased proliferative activity was directly proportionate to lymph node positivity for tumour invasion. A statistically significant correlation between MIB-1 expression and lymph node invasion in the examined prostatectomy cases with prostate cancer was found ($p<0.05$).

Table (25): *MIB-1 expression in relation to lymph node status in prostatectomy specimens:*

Patient group	MIB-1 expression		Total
	< 15 %	> 15 %	
Node-negative cases	21(70%)	9(30%)	30
Node-positive cases	2(28.6%)	5(71.4%)	7
Total	23	14	37

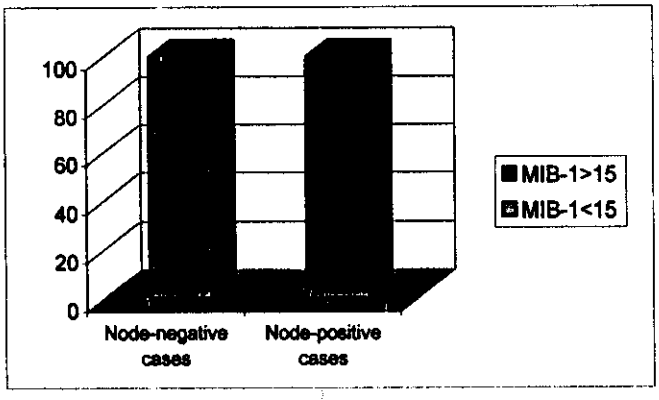

Graph(16): MIB-1 expression in relation to lymph node status in prostatectomy specimens.

p21 Results:

No immunolabeling was found in any of the negative controls. Intense immunostaining of the nuclei of malignant epithelial cells in invasive duct carcinoma of the breast used as a positive control tissue (Fig. 38).

Immunohistochemical staining of $p21^{WAF1}$ was observed exclusively in the nuclei. In noncancerous lesions, $p21^{WAF1}$ immunostaining was mostly detected in the luminal layer of prostatic acini . In adenocarcinoma, $p21^{WAF1}$ expression was focal or scattered and likely to be detected in well-differentiated areas.

Analysis of $p21^{WAF1}$ protein in prostatic carcinoma:

$p21^{WAF1}$ –positive tumour cells ranged from 1% to 75 %. Median value was 10 *(Table 26)*. The specimen showing > 10% of $p21^{WAF1}$ positive tumour cell nuclei were defined as positive and as being negative if it showed p21 positivity < 10%.

Out of the studied 100 cases, there were 53 (53%) p21-positive cases, while; the remaining 47 cases (47%) were negative for p21 immunoreactivity.

Table(26)Distribution of p21 expression in examined prostate cancer cases:

p21 expression	*No. of cases*	*Percentage*
Negative	*35*	*35%*
<10%	*12*	*12%*
10-25%	*40*	*40%*
25-50%	*5*	*5%*
>50%	*8*	*8%*
Total	*100*	*100%*

Correlation between histopathologic pattern and p21 immunoreactivity :

Out of the 15 cases with pattern 2 , 7 cases(46.7%) showed positive p21 immunoreactivity and 8 (53.3%) showed negative p21 immunoreactivity.

Out of the 42 cases with pattern 3, 33 cases(78.6%) showed positive p21 immunoreactivity and 9 (21.4%) showed negative p21 immunoreactivity.

Out of the 29 cases with pattern 4, 10 cases(34.5%) showed positive p21 immunoreactivity and 19 (65.5%) showed negative p21 immunoreactivity.

Out of the 14 cases with pattern 5, 3 cases (21.4%) showed positive p21 immunoreactivity and 11 (78.6%) showed negative p21 immunoreactivity.

This means; the worse the histopathologic pattern, the more the negativity of p21 expression *(Table,27)*. A high statistically significant inverse correlation between histopathologic pattern and p21 immunoreactivity was detected*(P<0.01)*.

Table(27):Correlation between p21 immunoreactivity and pathologic patterns:

Histopathologic pattern	p21 expression		Total
	+ve	-ve	
Pattern 2	7(46.7%)	8(53.3%)	15
Pattern 3	33(78.6%)	9(21.4%)	42
Pattern 4	10(34.5%)	19(65.5%)	29
Pattern 5	3(21.4%)	11(78.6%)	14
Total	53	47	100

Correlation between p21 expression and nuclear grade in studied cases:

Out of the 76 low-nuclear grade tumours(G1,G2),51 cases(67.1%) showed positive p21 immunoreactivity (Fig.39) and the remaining 25(32.9%) cases showed negative p21 immunoreactivity *(Table 28;Graph 17)*.

Two out of the 24 cases with nuclear G3 tumours (8.3%) showed positive p21 immunoreactivity and the remaining 22 cases(91.7%) showed negative p21 immunoreactivity .

So,the higher the nuclear grade, the more negative p21 expression.

A highly statistically significant inverse correlation between p21 expression and nuclear grade was found (P<0.01).

Table (28): p21 expression results according to nuclear grade in all cases:

Nuclear grade	p21 expression		Total
	+ve	-ve	
1	8(61.5%)	5(38.5%)	13
2	43(68.3%)	20(31.7%)	63
3	2(8.3%)	22(91.7%)	24
Total	53	47	100

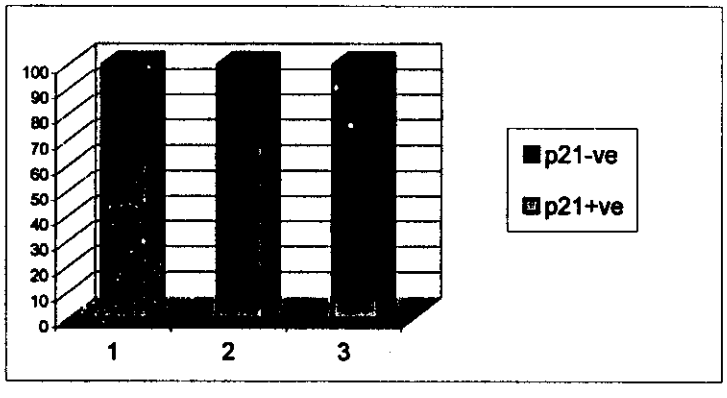

Graph(17):p21 expression in relation to nuclear grade in all cases.

Correlation between P21 expression and Gleason Sum Score in studied cases:

Ten out of 52 (19.2%) low-Gleason Sum Score tumours showed negative p21 immunoreactivity and the remaining 42 cases (80.8%) showed positive p21 immunoreactivity (Fig.40) *(Table 29;Graph 18).*

Thirty seven out of 48 (77.1%) high–Gleason Sum Score tumours showed negative p21 immunoreactivity (Fig.41) and the remaining 11 cases (22.9%) showed positive p21 immunoreactivity.

The number of p21-positive cases was significantly greater in low-grade tumours than in high –grade tumours .

This means, the higher the Gleason Sum Score, the more negative p21 expression.

There was a highly significant inverse correlation between p21 expression and G.S.Score ($P<0.01$).

Table (29): p21 expression results according to Gleason Sum Score in all cases:

G.S.S.	p21 Expression		Total
	+ve	-ve	
< 7	42(80.8%)	10(19.2%)	52
≥ 7	11(22.9%)	37(77.1%)	48
Total	**53**	**47**	**100**

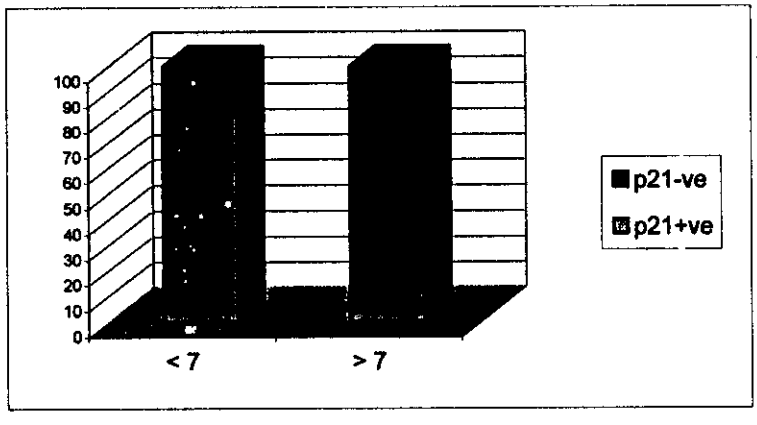

Graph(18):p21 expression in relation to G.S.Score in all cases.

Correlation between p21 expression and pathologic stage in prostatectomy specimens:

Out of the 18 cases of pT2, 13 cases (72.2%) showed positive immunoreaction to p21, and 5 (27.8%) showed negative immunoreaction to p21 *(Table 30;Graph 19)*.

Eight out of the 12 cases of pT3 (66.7%) showed positive immunoreaction to p21, and 4 (33.3%) showed negative immunoreaction to p21 .

Of the 7 cases of pT4, 2 cases (28.6%) showed positive immunoreaction to p21, and 5 (71.4%) showed negative immunoreaction to p21 .

So,the higher the stage, the more negative p21 expression.

An inverse correlation;though statistically insignificant,between p21 immunoreactivity and pathologic stage was found *(p>0.01)*.

Table (30): Pathologic stage in relation to p21 positivity in prostatectomy specimens:

pT – stage	p21 expression		Total
	+ve	-ve	
pT-2	13(72.2%)	5(27.8%)	18
pT-3	8(66.7%)	4(33.3%)	12
pT-4	2(28.6%)	5(71.4%)	7
Total	23	14	37

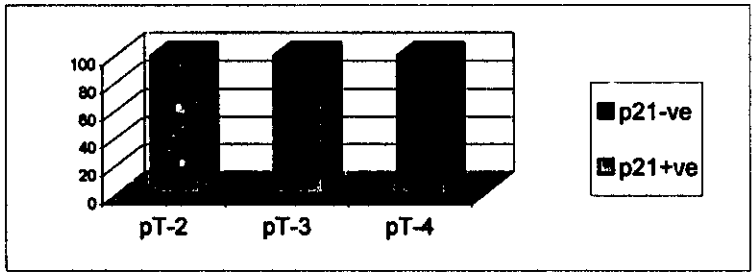

Graph(19):Pathologic stage in relation to p21 positivity in prostatectomy specimens.

p21 expression in relation to lymph node status in prostatectomy specimens:

In prostatectomy specimens,out of the 7 node-positive cases, 2 cases (28.6%) showed positive p21 immunoreactivity and 5 cases (71.4%) showed negative p21 immunoreactivity,while in the 30 node-negative cases,21 cases(70%)showed positive p21 immunoreactivity and 9 cases (30%) showed negative p21 immunoreactivity *(Table 31;Graph 20)*.

The 2 cases with positive p21 immunoreactivity were of low-G.S.Score (G.S. 5,6).

There was an inverse, though statistically insignificant, correlation between p21 immunoreactivity and lymph node positivity for tumour invasion *($p>0.01$)*.

Table (31): *p21 expression in relation to lymph node status in prostatectomy specimens:*

Patient group	p21 expression		Total
	+ve	-ve	
Node-negative cases	21(70%)	9(30%)	30
Node-positive cases	2(28.6%)	5(71.4%)	7
Total	23	14	37

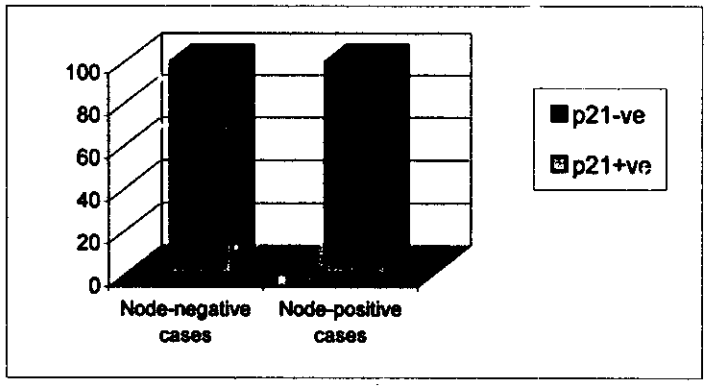

Graph(20): p21 expression in relation to lymph node status in prostatectomy specimens.

Correlation between markers expression:

Correlation between CD44 expression and p21 expression in all cases:

Out of the 42 cases with CD44 expression <10%, 13 cases (31%) showed positive p21 immunoreactivity and 29 cases (69%) were negative.

Out of the 58 cases with CD44 expression >10% , 40 cases (69%) showed positive p21 immunoreactivity and 18 cases (31%) were negative.

So, decreased CD44 expression is proportionate to p21 negativity. Statistically, a highly significant correlation between CD44 expression and p21 immunoreactivity was found ($p<0.01$) *(Table,32;Graph,21).*

Table (32):Correlation between CD44 expression and p21 expression in all cases:

CD44 expression	p21 Expression		Total
	+ ve	- ve	
<10%	13(31%)	29(69%)	42
>10%	40(69%)	18(31%)	58
Total	53	47	100

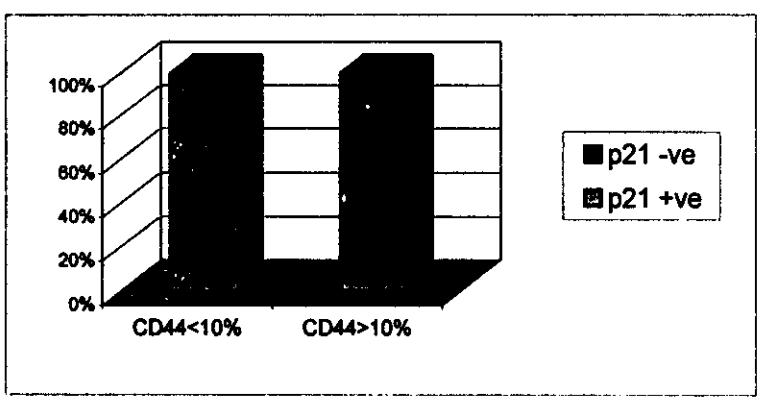

Graph(21):CD44 expression in relation to p21 immunoreactivity in all cases.

Correlation between CD44 expression and MIB-1 expression in all cases:

Out of the 58 cases with CD44 expression >10%, 44 cases (75.9%) showed MIB-1 expression <15% and 14 cases (24.1%) showed MIB-1 expression >15% *(Table 33 ;Graph 22).*

Out of the 42 cases with CD44 expression <10%, 29 cases (69%) showed MIB-1 expression <15% and 13 cases (31%) showed MIB-1 expression >15%.

So, the higher the proliferative activity of the tumour, the more reduction of CD44 expression.

It was found that MIB-1 expression was inversely correlated with CD44 expression, but this was statistically insignificant *(P>0.01).*

Table (33):Correlation between MIB-1 expression and CD44 expression in all cases:

MIB-1 expression	CD44 expression		Total
	< 10 %	> 10%	
<15%	29(69%)	44(75.9%)	73
>15%	13(31%)	14(24.1%)	27
Total	42	58	100

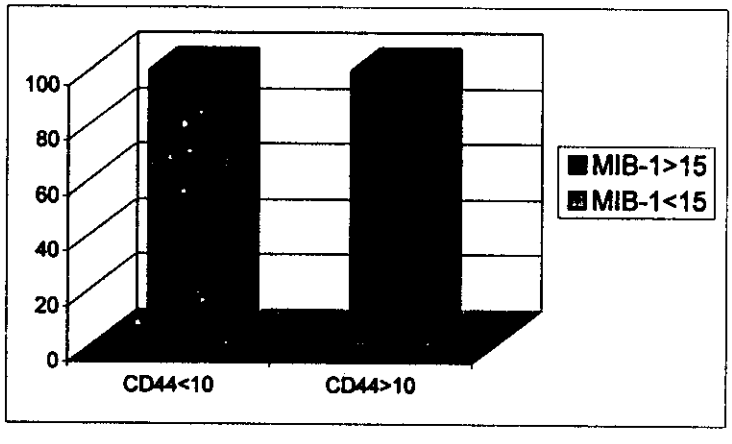

Graph(22):CD44 expression in relation to MIB-1 expression in all cases.

Correlation between p21 immunoreactivity and MIB-1 expression in all cases:

Out of the 53 cases with positive p21 immunoreactivity,40 cases (75.5%) showed MIB-1 expression <15% and 13 cases (24.5%)showed MIB-1 expression >15%.

Out of the 47 cases with negative p21 immunoreactivity ,33 cases (70.2%) showed MIB-1 expression <15% and 14cases (29.8%)showed MIB-1 expression >15%*(Table,34;Graph ,23).*

Thus MIB-1 expression correlated inversely with p21 immunoreactivity, although this was statistically insignificant .

Table (34): MIB-1 expression in relation to p21 immunoreactivity in all cases:

MIB-1 expression	p21 immunoreactivity		Total
	+ve	-ve	
<15%	40(75.5%)	33(70.2%)	73
>15%	13(24.5%)	14(29.8%)	27
Total	53	47	100

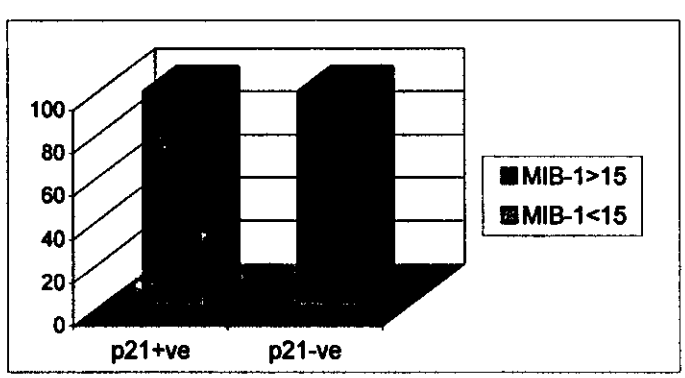

Graph(23):p21 immunoreactivity in relation to MIB-1 expression in all cases.

Correlation between markers expression and pathologic patterns : *Table(35).*

Regarding CD44 expression, it was found that 17 out of 42 cases(40.5%) that showed CD44 expression <10% were of patterns with lower grades; while, 25 cases(59.5%) were of patterns with higher grades.

Regarding MIB-1 expression, it was found that 43 out of 73 cases(58.9%) that showed MIB-1 expression <15% were of patterns with lower grades; while, 30 cases(41.1%) were of patterns with higher grades.

Regarding p21 immunoreactivity, it was found that 17 out of 47 cases(36.2%) that showed negative p21 immunoreactivity were of patterns with lower grades; while, 30 cases(63.8%) were of patterns with higher grades.

So, of the forementioned correlations, only the correlation between p21 immunoreactivity and histopathologic pattern was statistically significant (P<0.01).

Table(35):Correlation between markers expression and pathologic patterns:

Histopathologic pattern	CD44 expression		MIB-1 expression		p21 expression	
	<10%	>10%	<15%	>15%	+ve	-ve
Pattern 2	5(33.3%)	10(66.7%)	10(66.7%)	5(33.3%)	7(46.7%)	8(53.3%)
Pattern 3	12(28.6%)	30(71.4%)	33(78.6%)	9(21.4%)	33(78.6%)	9(21.4%)
Pattern 4	20(69%)	9(31%)	21(72.4%)	8(27.6%)	10(34.5%)	19(65.5%)
Pattern 5	5(35.7%)	9(64.3%)	9(64.3%)	5(35.7%)	3(21.4%)	11(78.6%)
Total	42	58	73	27	53	47

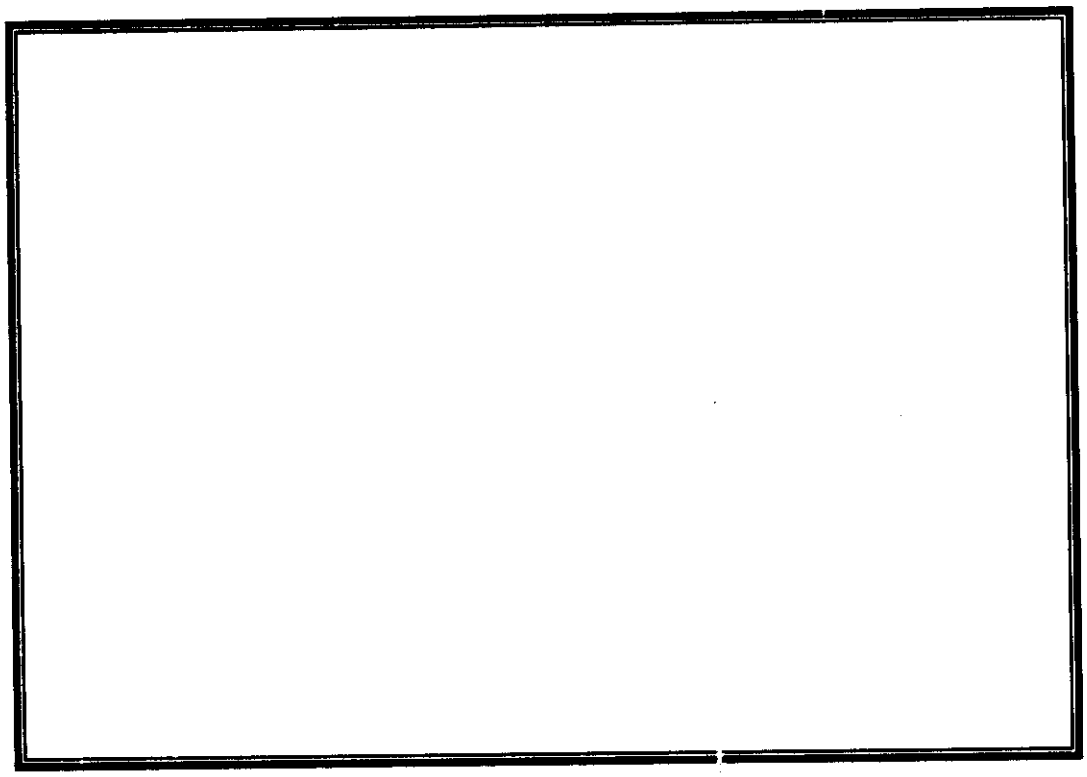

Fig (10): High-grade PIN- tufting pattern showing undulating mounds and heaps of cells protruding into the lumen. The basal cell layer is still intact (H&E x400).

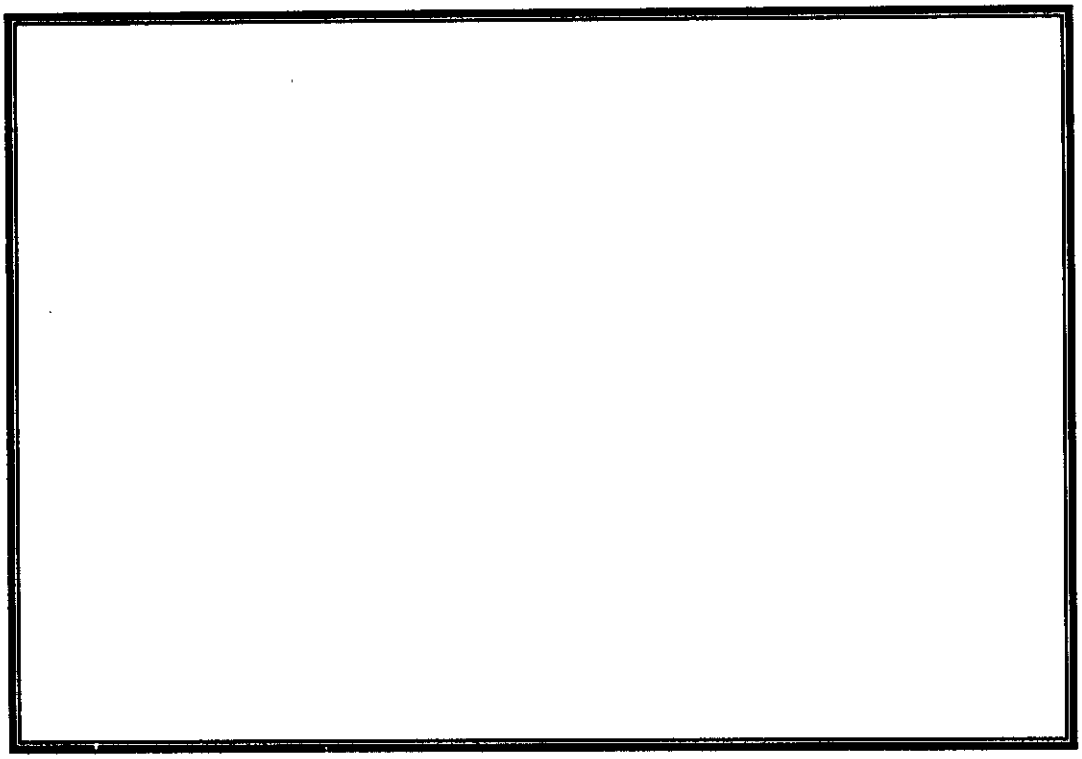

Fig. (11): High-grade PIN- papillary pattern showing finger-like projections lacking fibrovascular cores (H&Ex40).

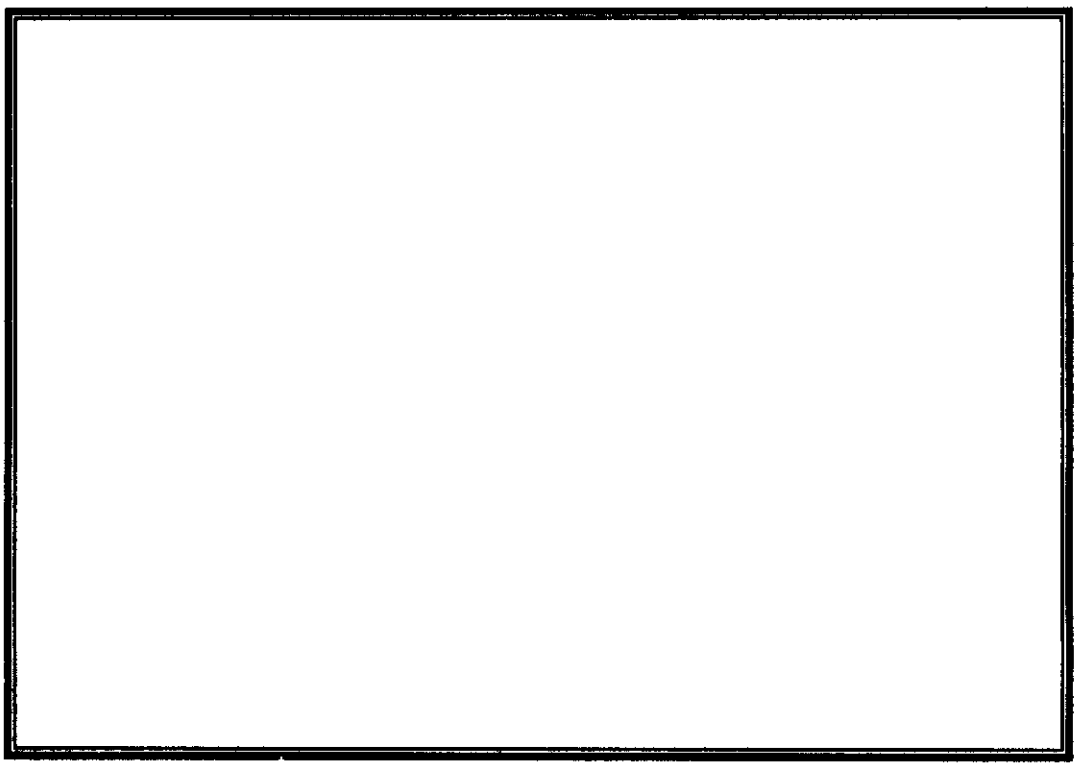

Fig. (12): High-grade PIN - cribriforming pattern, showing intraluminal proliferation of cells punctated by multiple lumens, and cribriforming carcinoma (H&E x100).

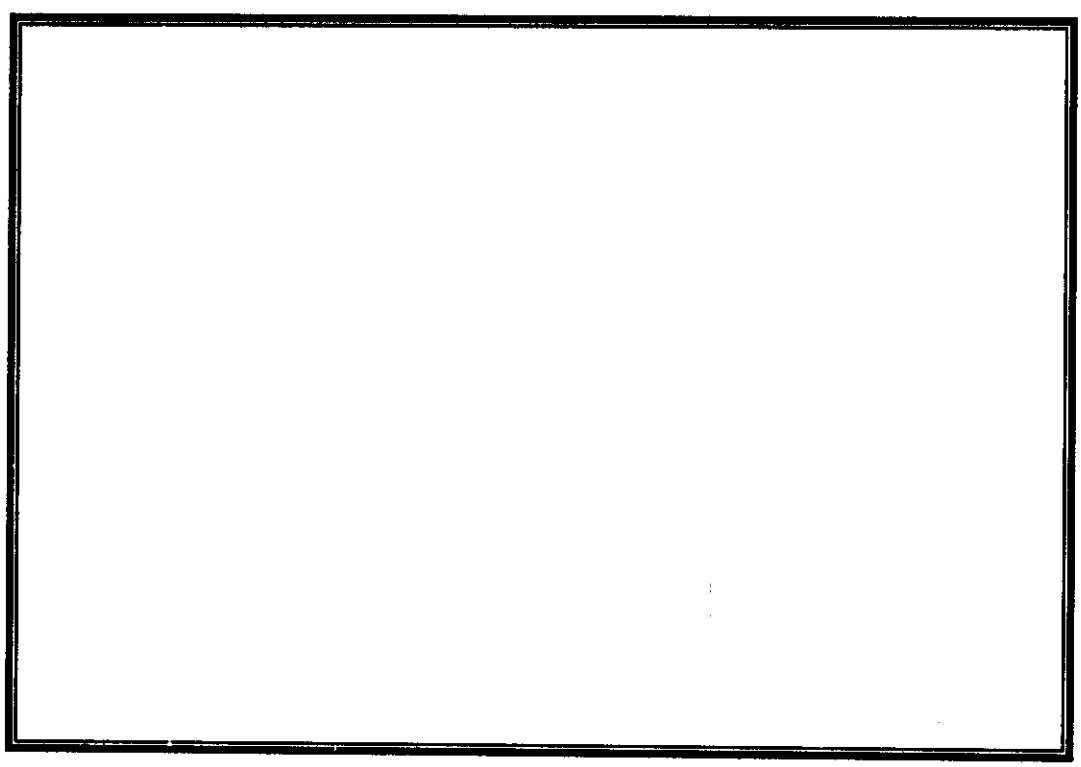

Fig. (13): High-grade PIN – flat pattern (H&E x100).

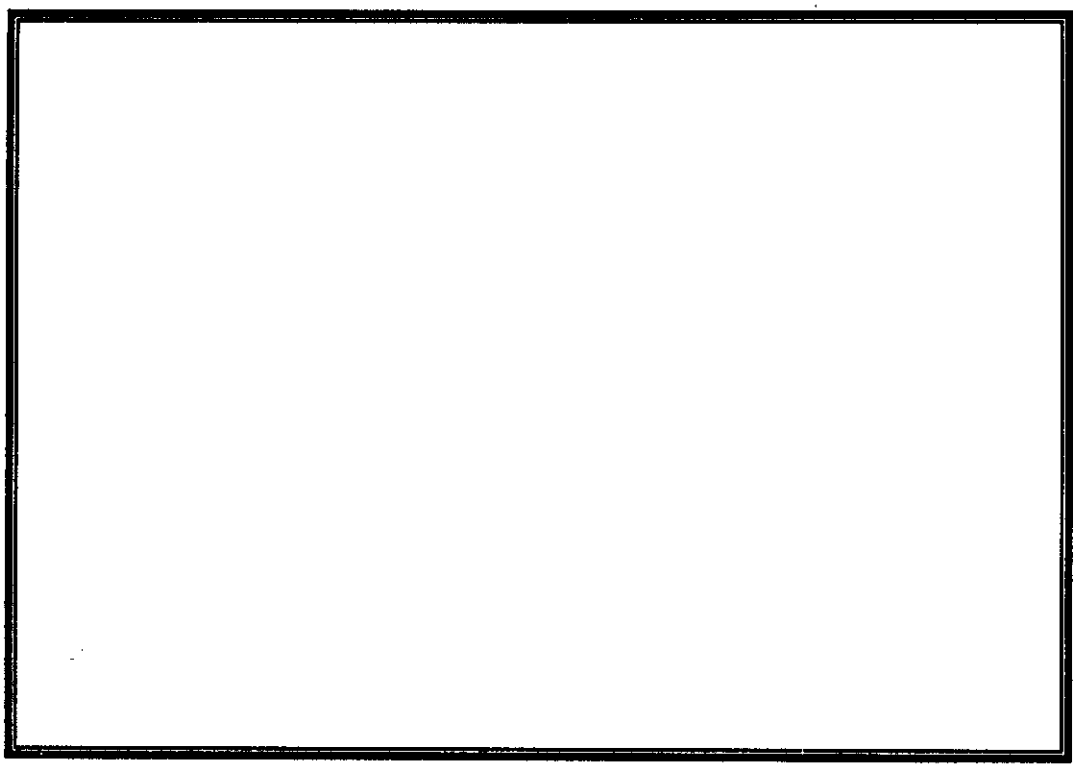

Fig. (14): Prostatic adenocarcinoma - pattern 2 showing fairly cicumscribed nodule with loosely arranged glands (H&E x40).

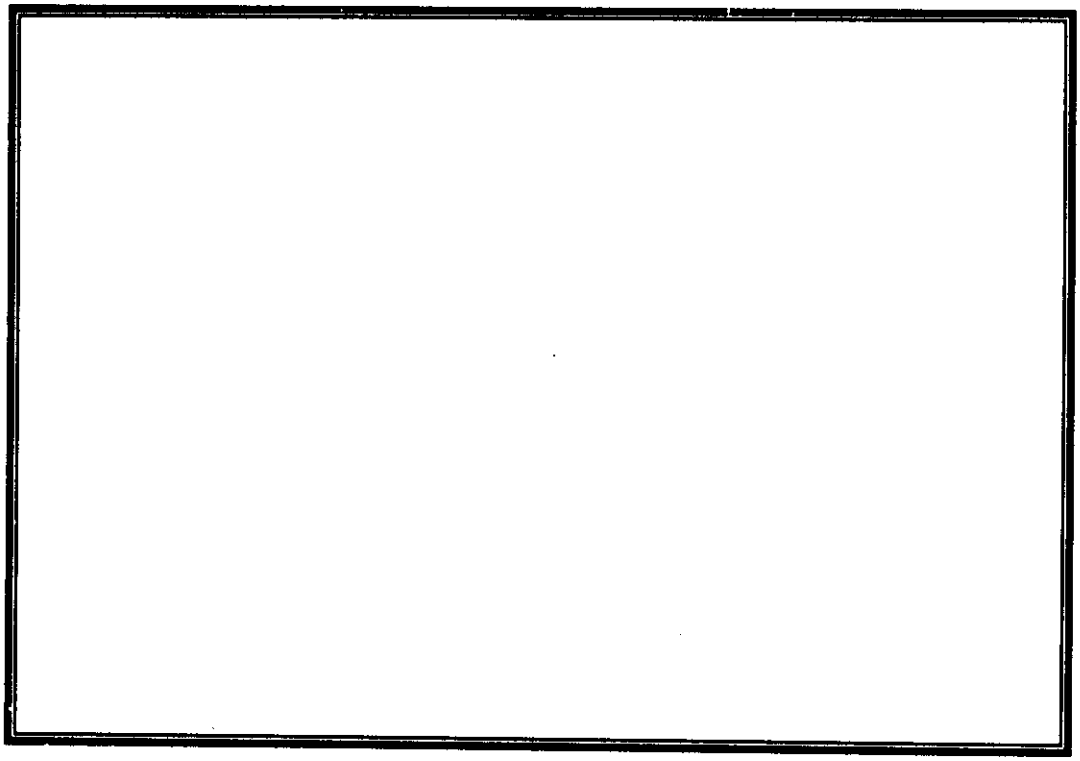

Fig. (15): Prostatic adenocarcinoma - pattern 3 glands showing variable-sized and shaped glands with infilterative appearance among larger benign glands (H&E x40).

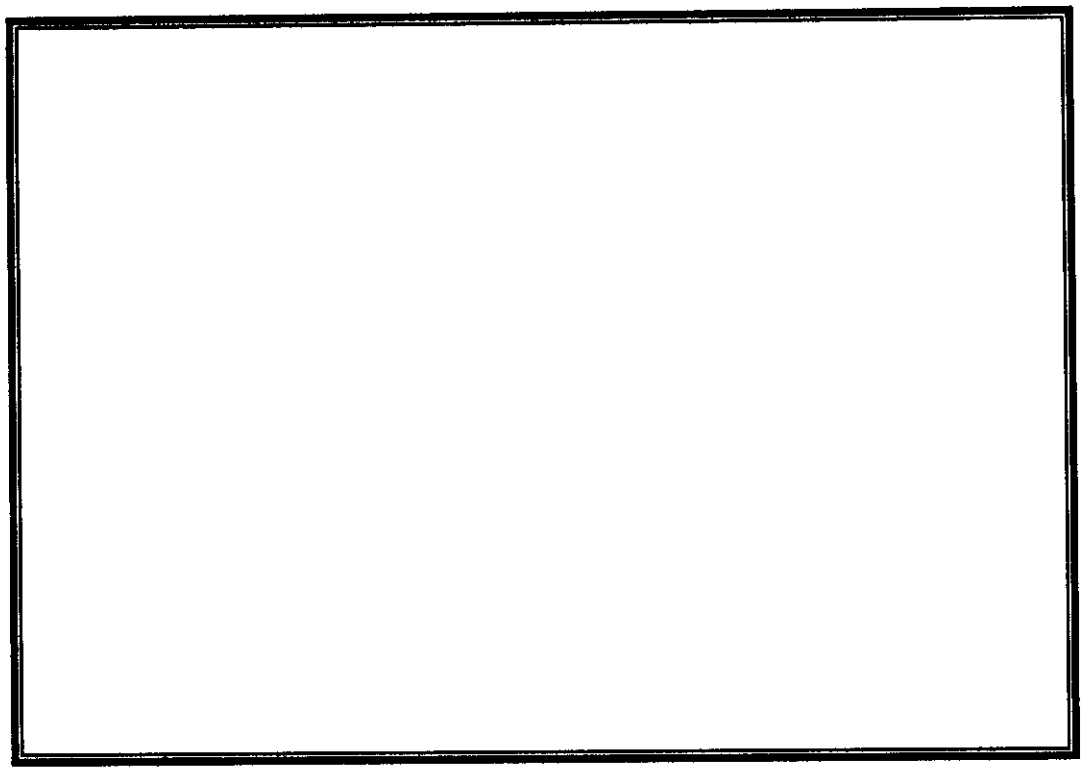

Fig. (16): Prostatic adenocarcinoma – papillary pattern showing rounded masses of papillary epithelium (H&E x100).

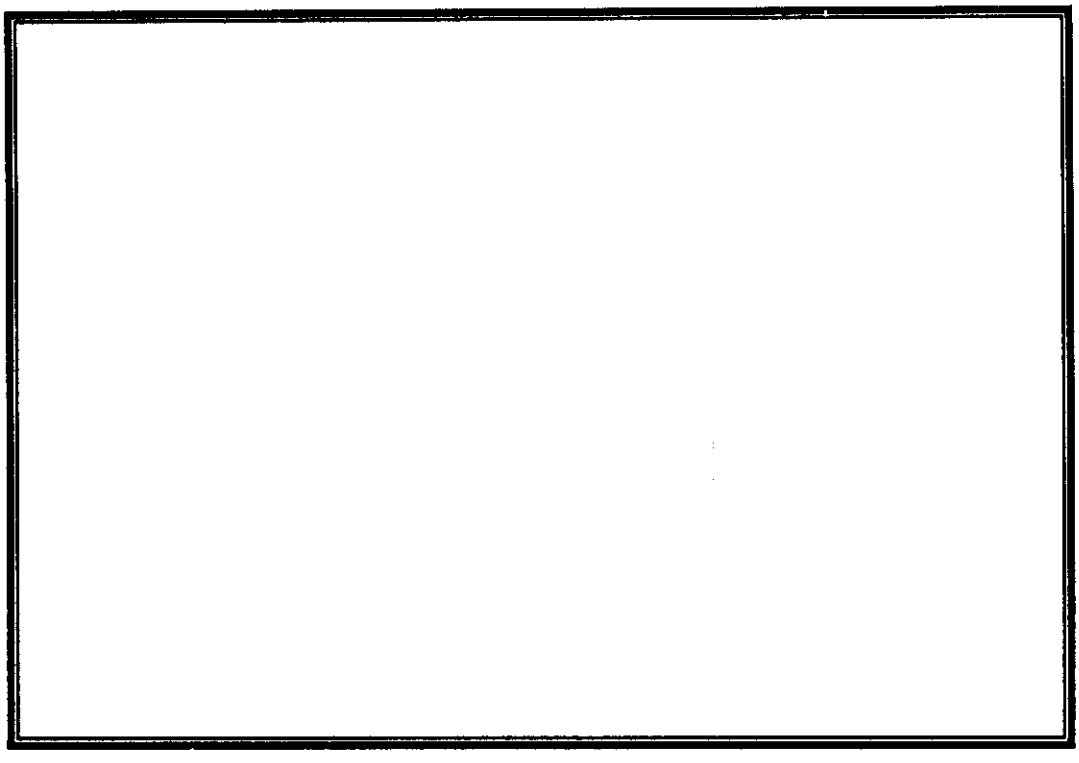

Fig. (17): Prostatic adenocarcinoma – fused glands pattern with the glands are no longer single and separate (H&E x100).

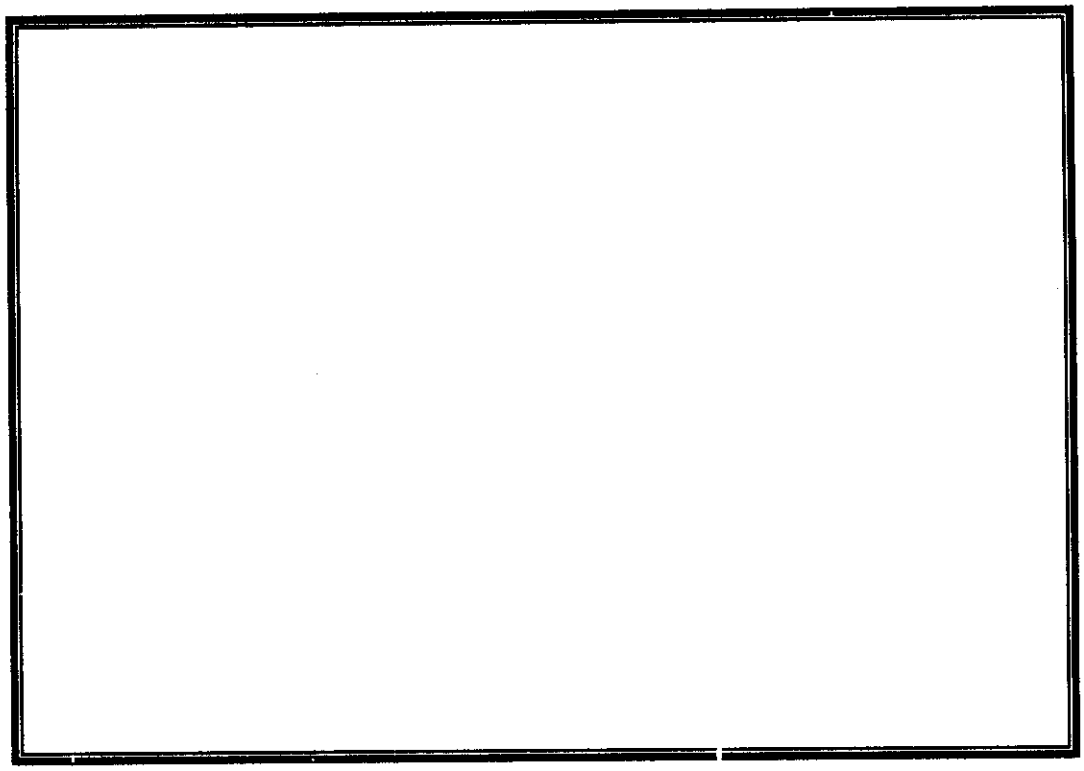

Fig. (18): Prostatic adenocarcinoma – clear cell pattern showing large pale hypernephroid cells (H&E x100).

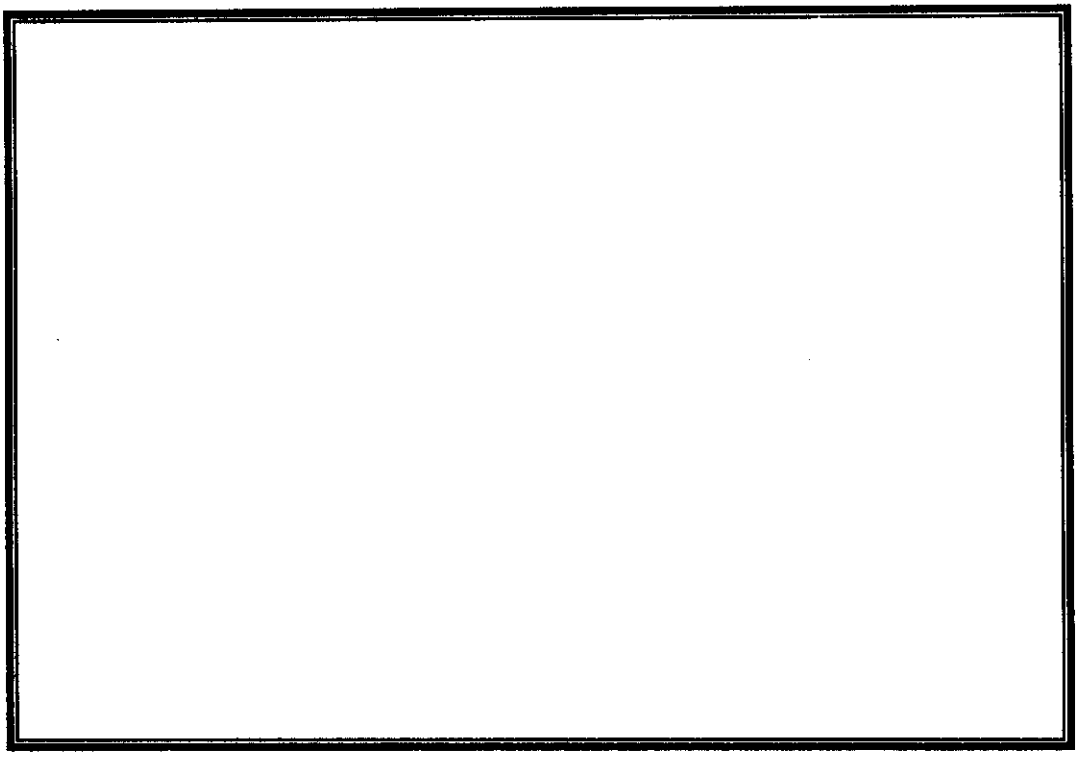

Fig. (19): Prostatic adenocarcinoma showing comedo necrosis in the form of large cribriforming masses with central necrosis (H&E x40).

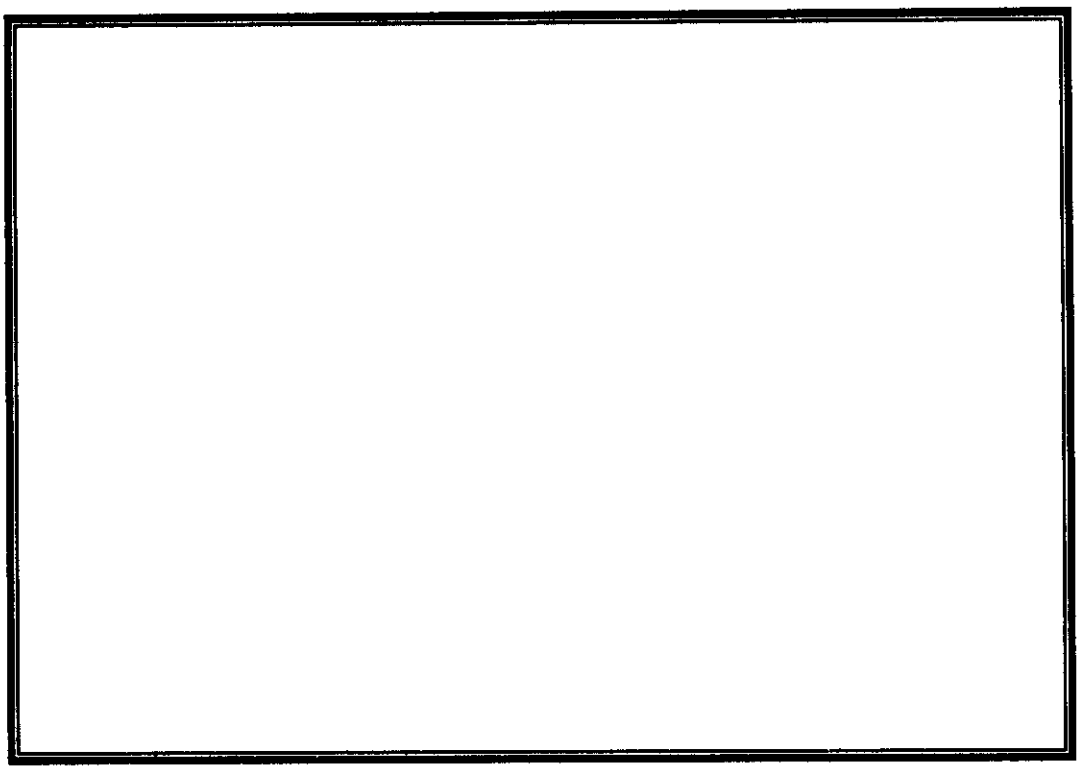

Fig. (20): Prostatic adenocarcinoma – anaplastic pattern showing solid masses of cells with no glandular differentiation (H&E x200).

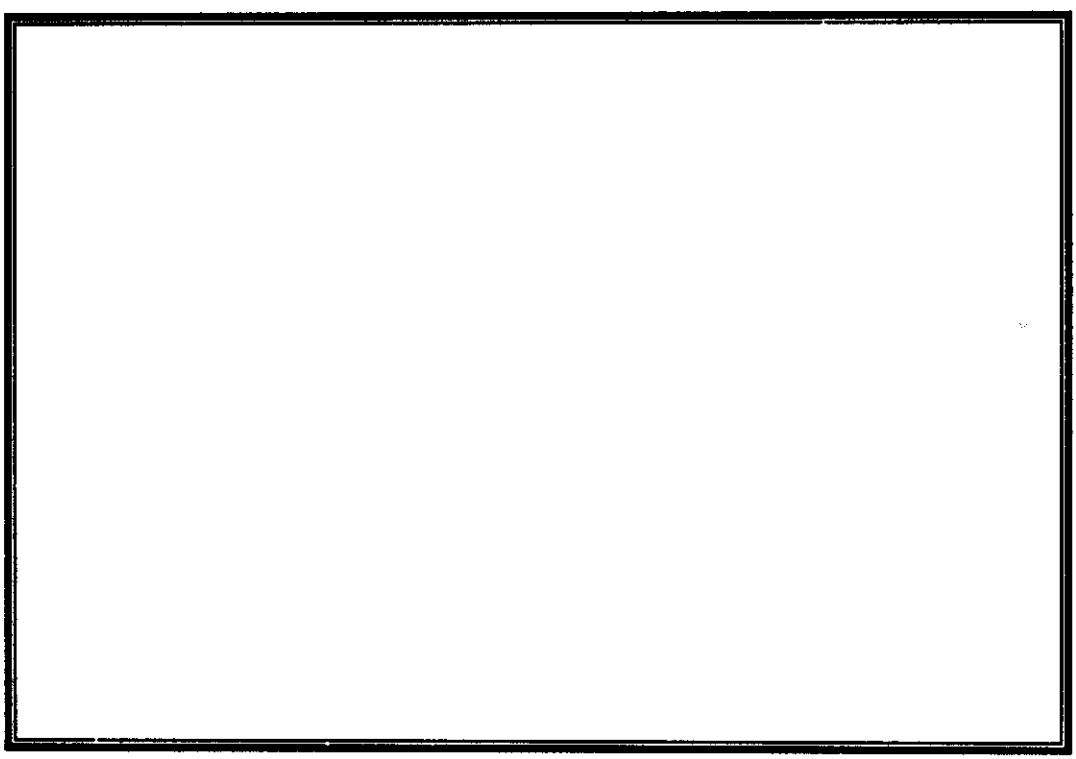

Fig. (21): Prostatic adenocarcinoma – mucoid carcinoma pattern with the malignant glands floating within pools of mucin(H&E x100).

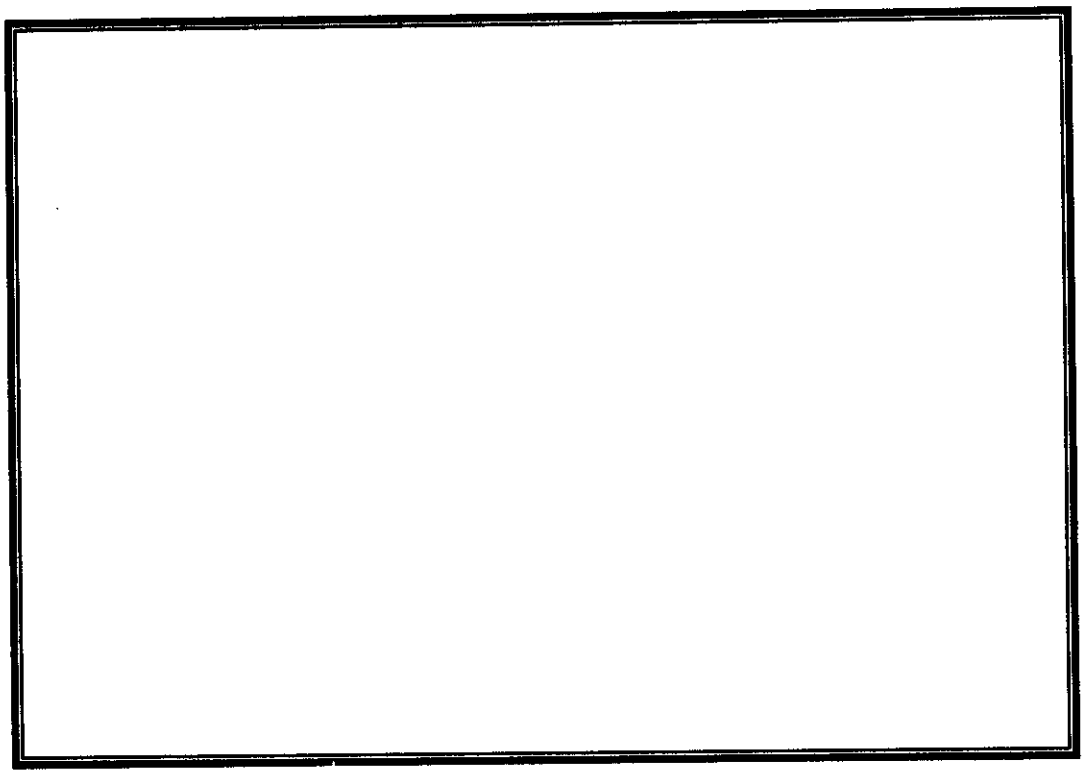

Fig. (22): Prostatic adenocarcinoma – neuroendocrine differentiation showing oesinophilic granular cytoplasm and luminal differentiation (H&E x200).

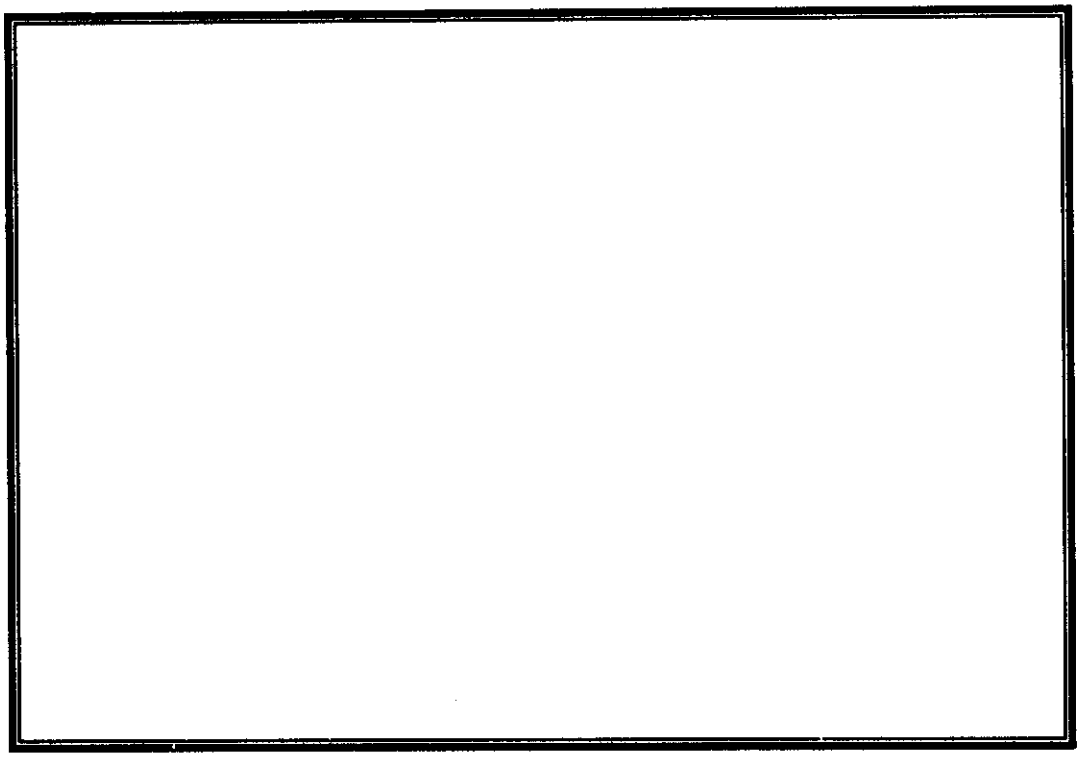

Fig. (23): Prostatic adenocarcinoma showing perineural invasion by malignant glands that are seen within the neural sheath (H&E x100).

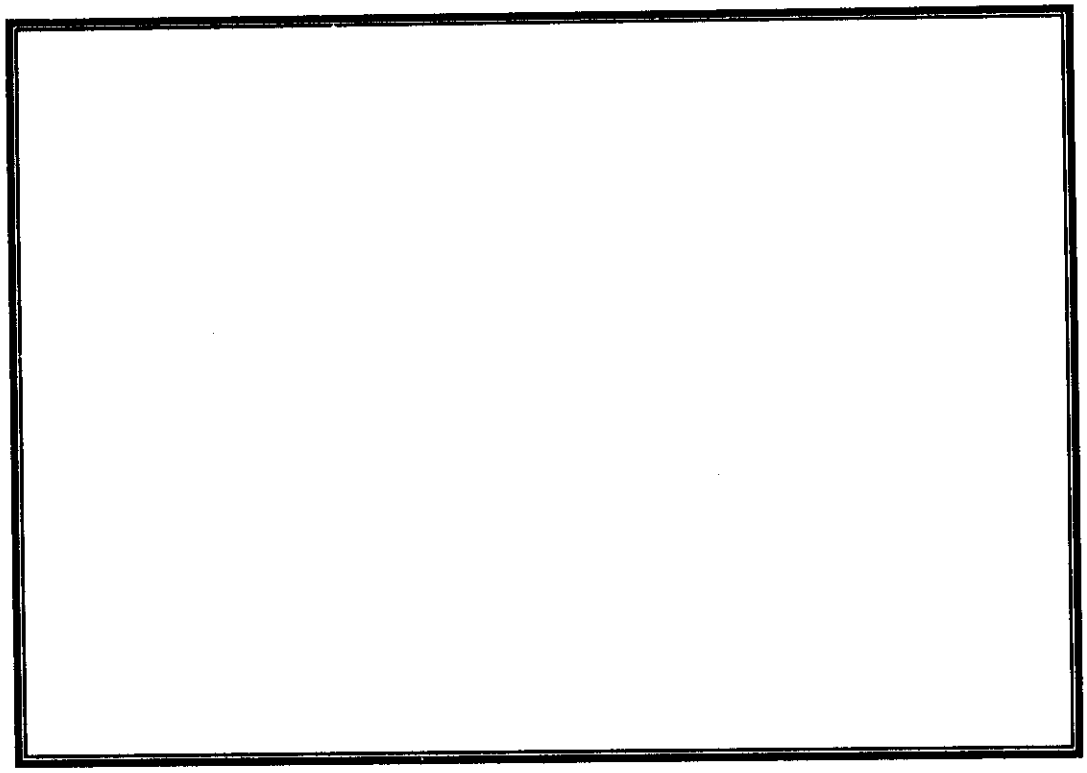

Fig. (24): Prostatic adenocarcinoma showing vascular embolization by malignant cells (H&E x200).

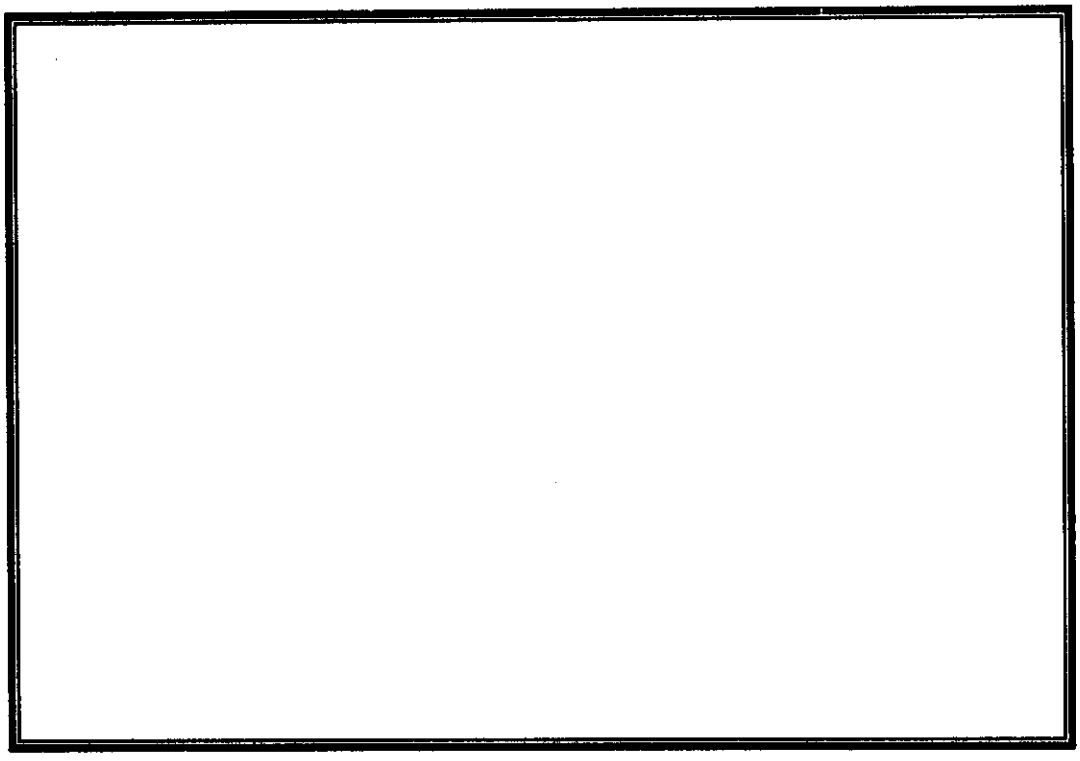

Fig. (25): Prostatic adenocarcinoma showing capsular penetration (H&E x??).

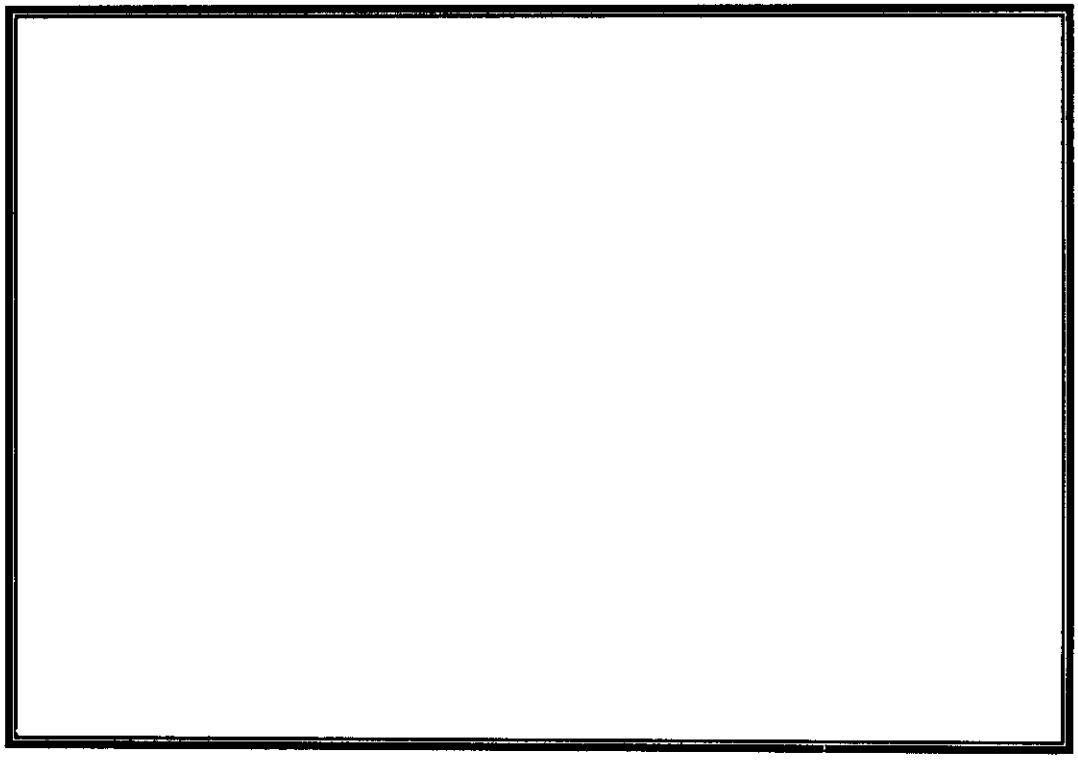

Fig. (26): Normal skin showing positive CD44 expression as a control (Streptavidin-Biotin x200).

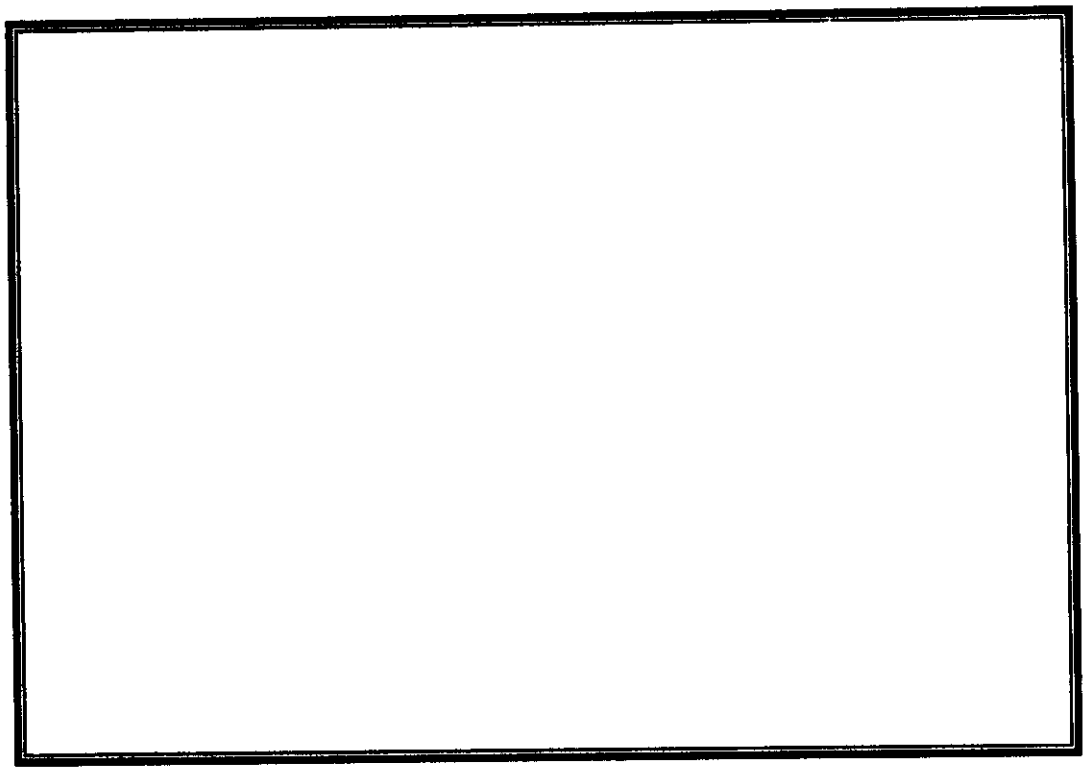

Fig. (27): Low-grade prostatic adenocarcinoma (G.S.S. 6, G2) showing membranous CD44 expression >10% (Streptavidin-Biotin x200).

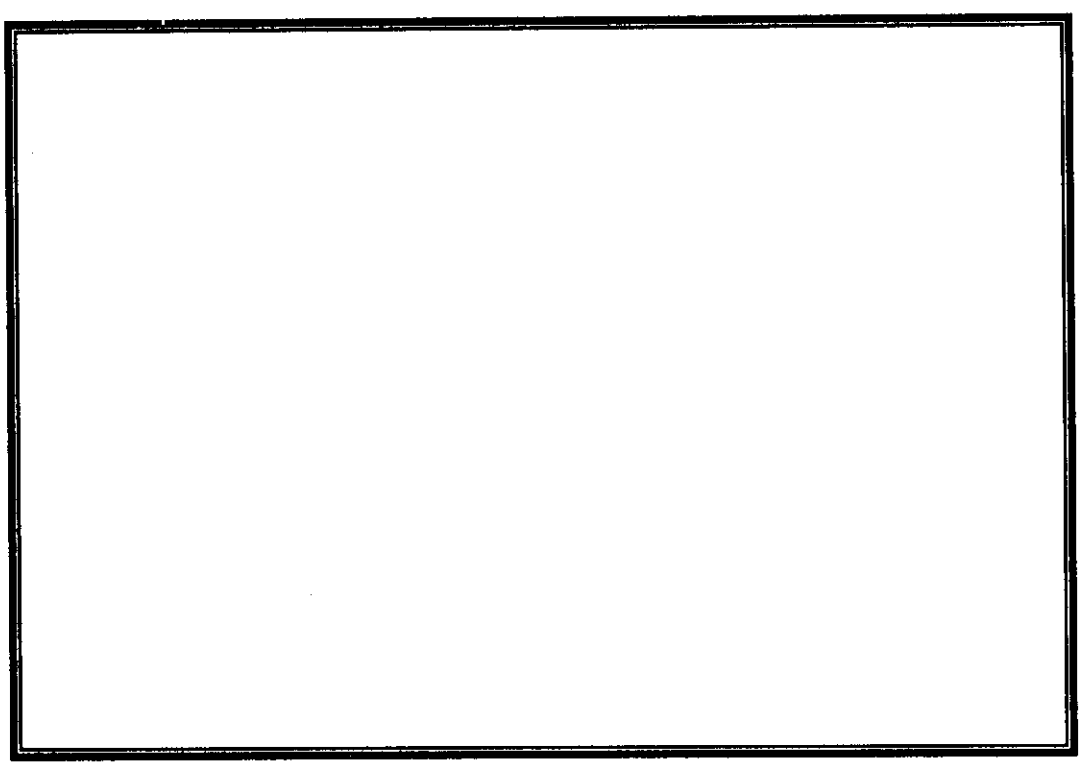

Fig. (28): Low-grade prostatic adenocarcinoma (G.S.S. 6, G2) showing membranous CD44 expression >10% (Streptavidin-Biotin x200).

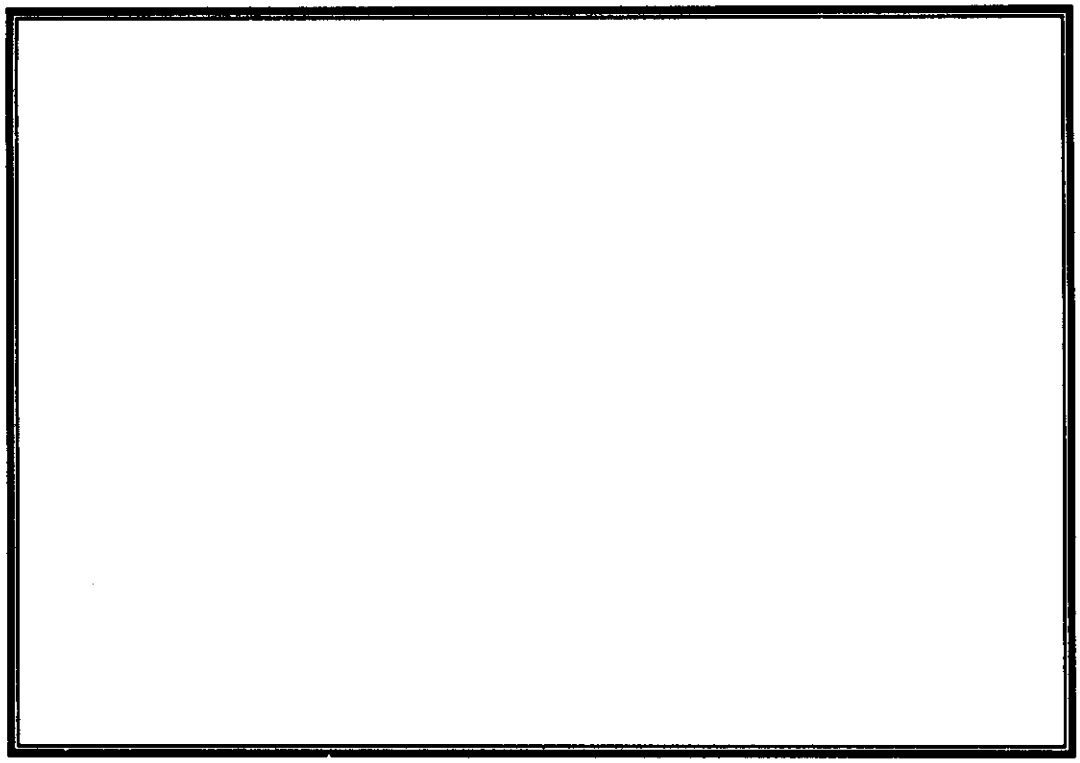

Fig. (29): High-grade prostatic adenocarcinoma (G.S.S. 7, G2) showing membranous CD44 expression <10% (Streptavidin-Biotin x200).

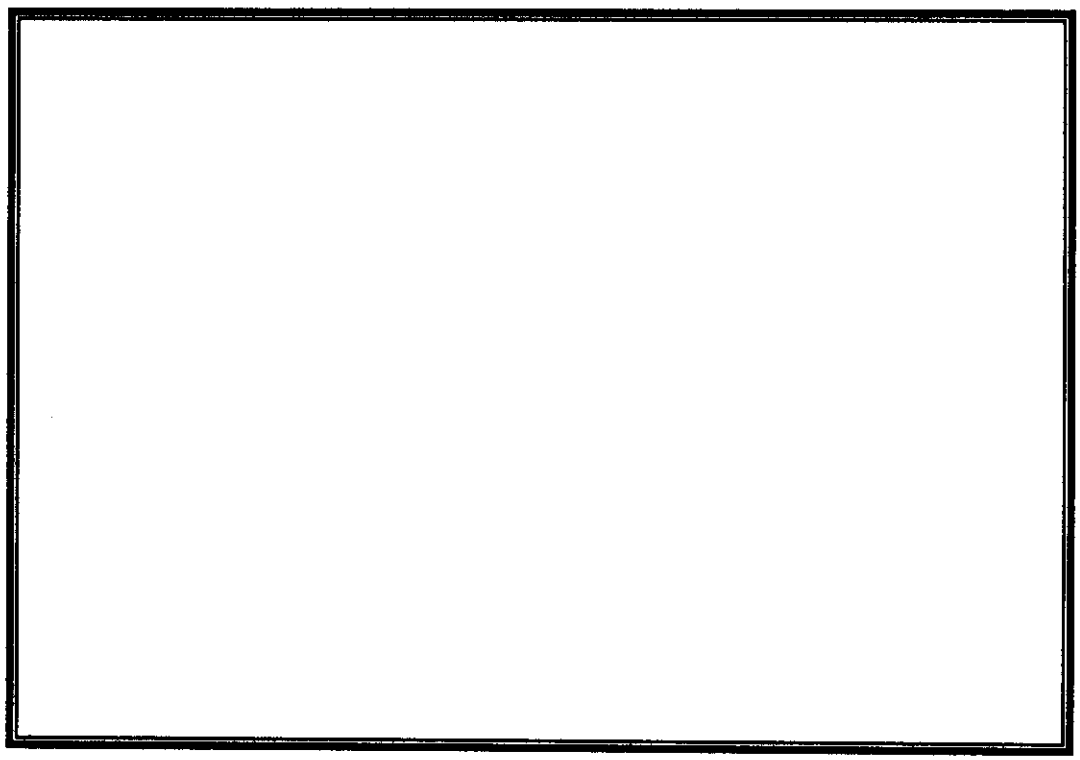

Fig. (30): High-grade prostatic adenocarcinoma (G.S.S. 8, G2) showing absent CD44 expression with positive staining of lymphocytes as an internal control (Streptavidin-Biotin x100).

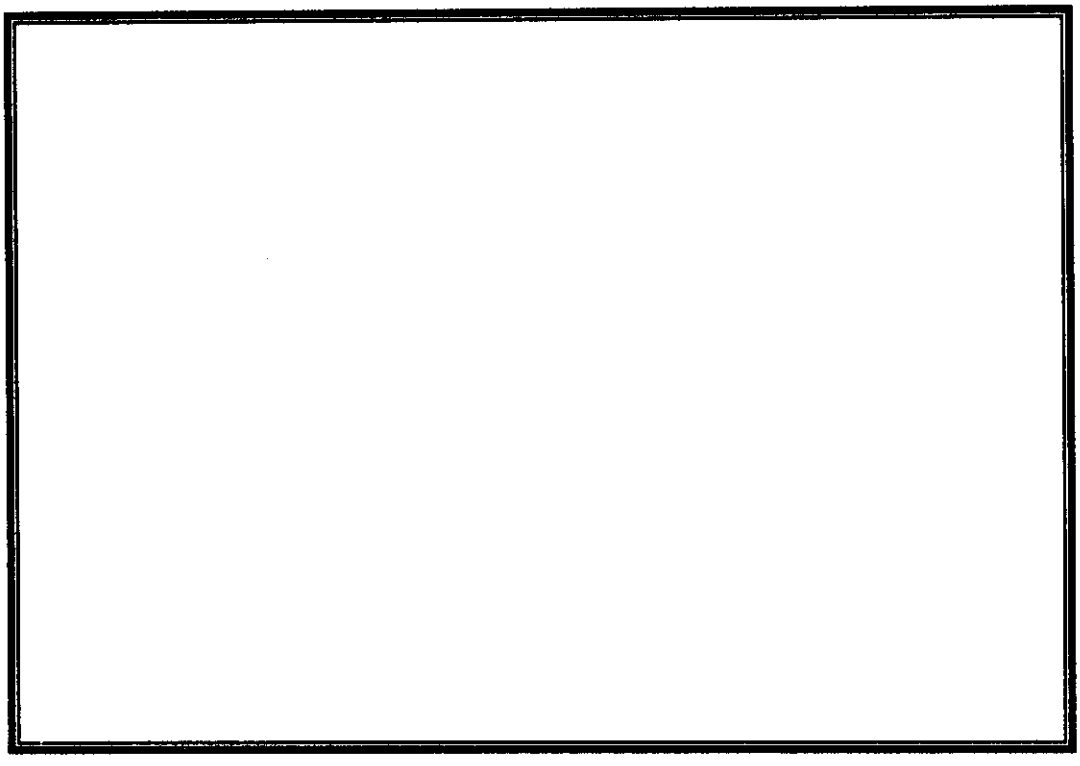

Fig. (31): Human tonsil showing positive MIB-1 expression as a control (Streptavidin-Biotin x200).

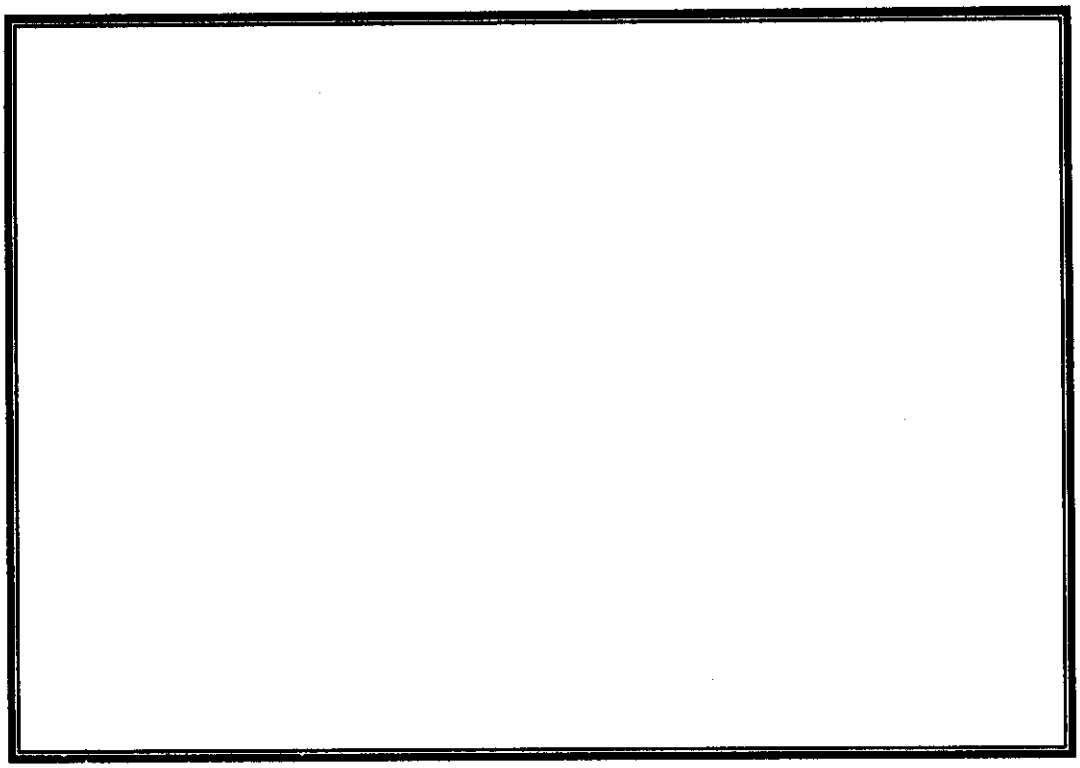

Fig. (32): High-grade prostatic adenocarcinoma with cribriforming pattern (G.S.S. 7, G2) showing high nuclear MIB-1 expression (Streptavidin-Biotin x200).

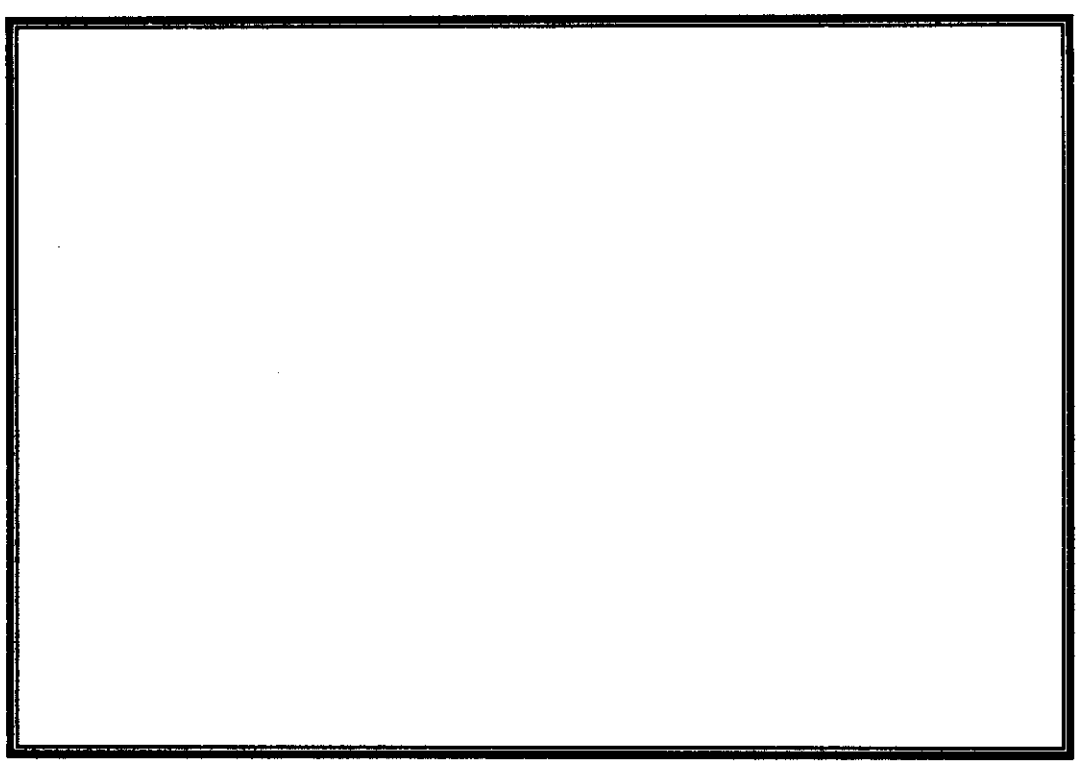

Fig. (33): High-grade prostatic adenocarcinoma with fused glands pattern (G.S.S. 7, G2) showing high nuclear MIB-1 expression (Streptavidin-Biotin x200).

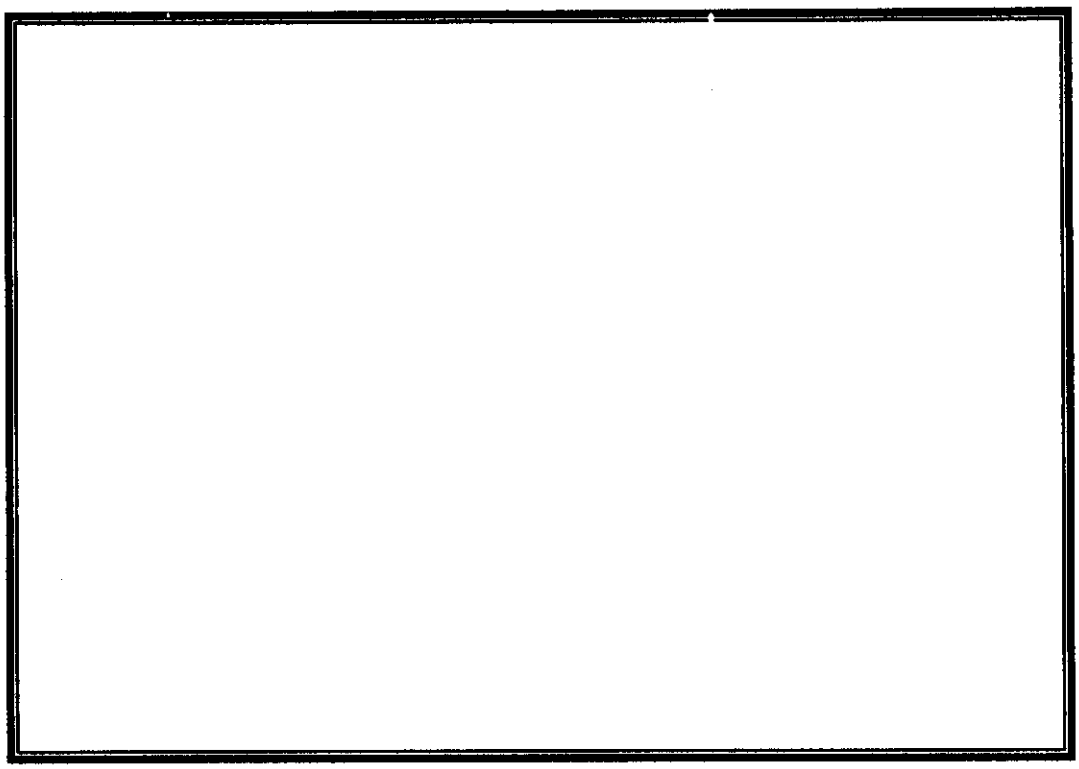

Fig. (34): High-grade prostatic adenocarcinoma with fused glands pattern (G.S.S. 8, G3) showing high nuclear MIB-1 expression (Streptavidin-Biotin x200).

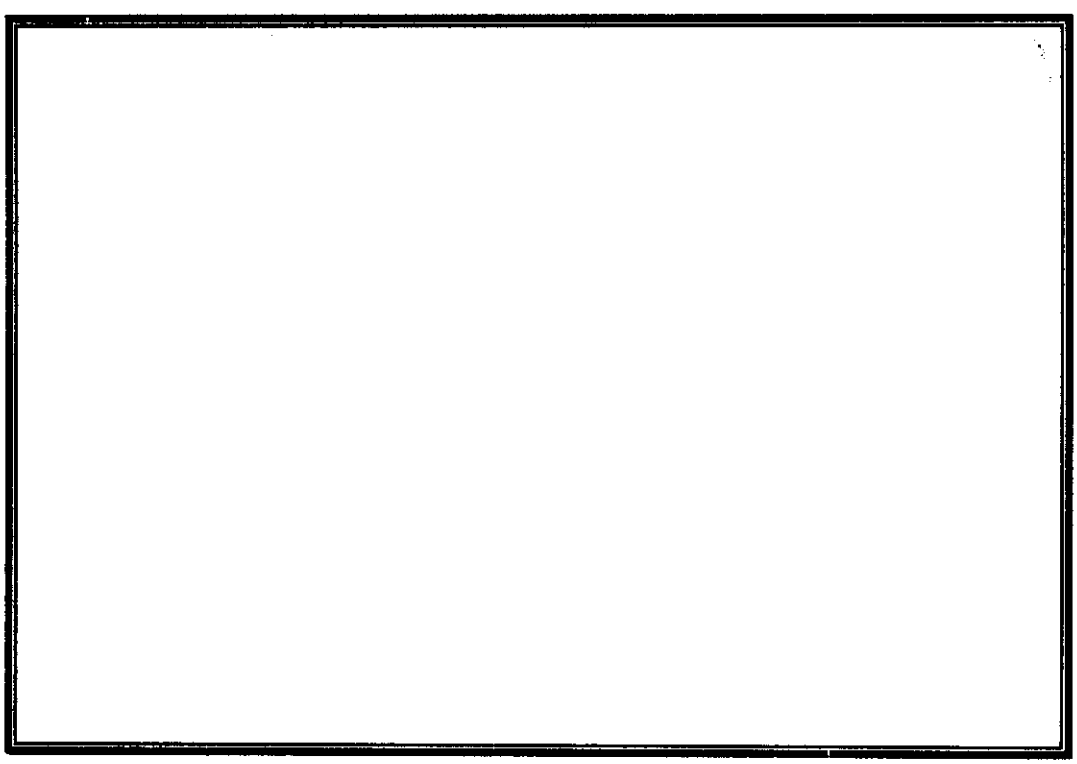

Fig. (35): High-grade prostatic adenocarcinoma – anaplastic pattern (G.S.S. 10, G3) showing high nuclear MIB-1 expression (Streptavidin-Biotin x200).

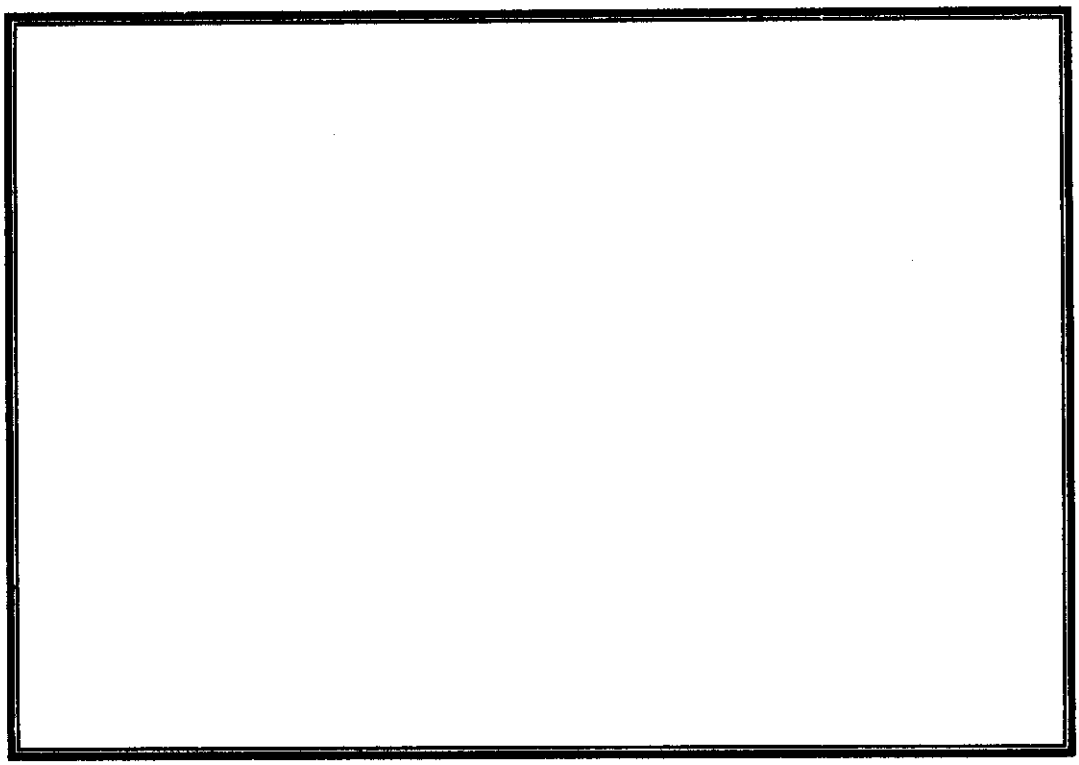

Fig. (36): Low-grade prostatic adenocarcinoma (G.S.S. 6, G2) showing low nuclear MIB-1 expression (Streptavidin-Biotin x200).

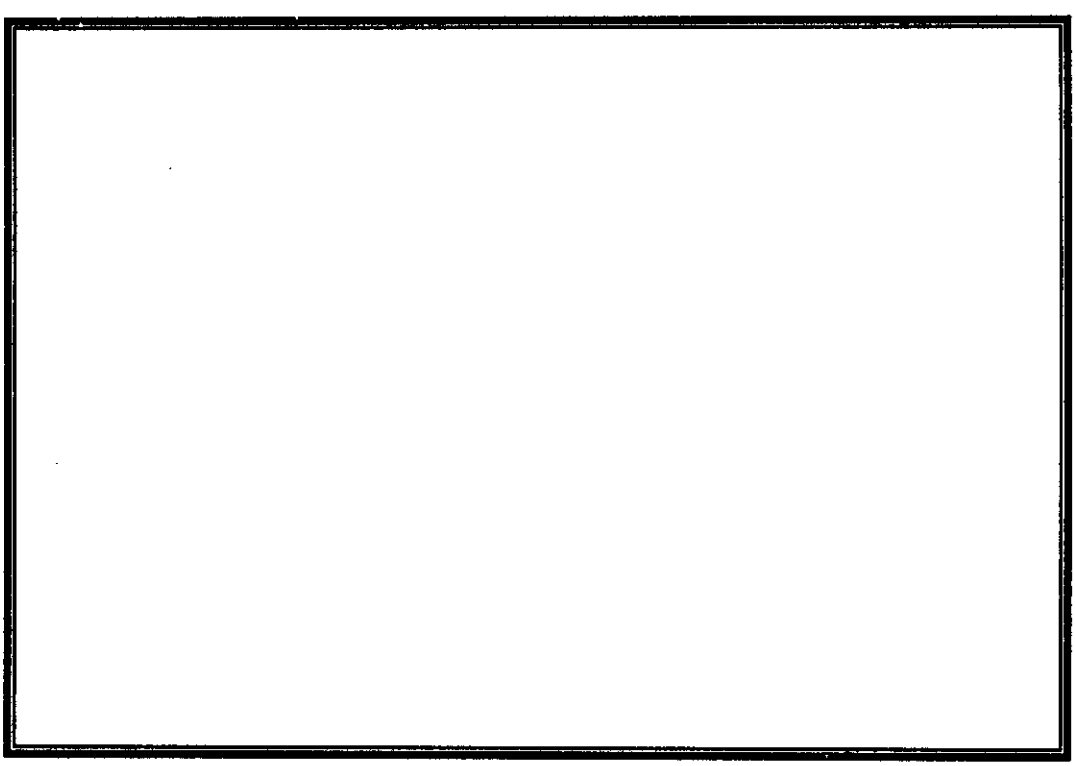

Fig. (37): Low-grade prostatic adenocarcinoma (G.S.S. 6, G2) showing low nuclear MIB-1 expression (Streptavidin-Biotin x200).

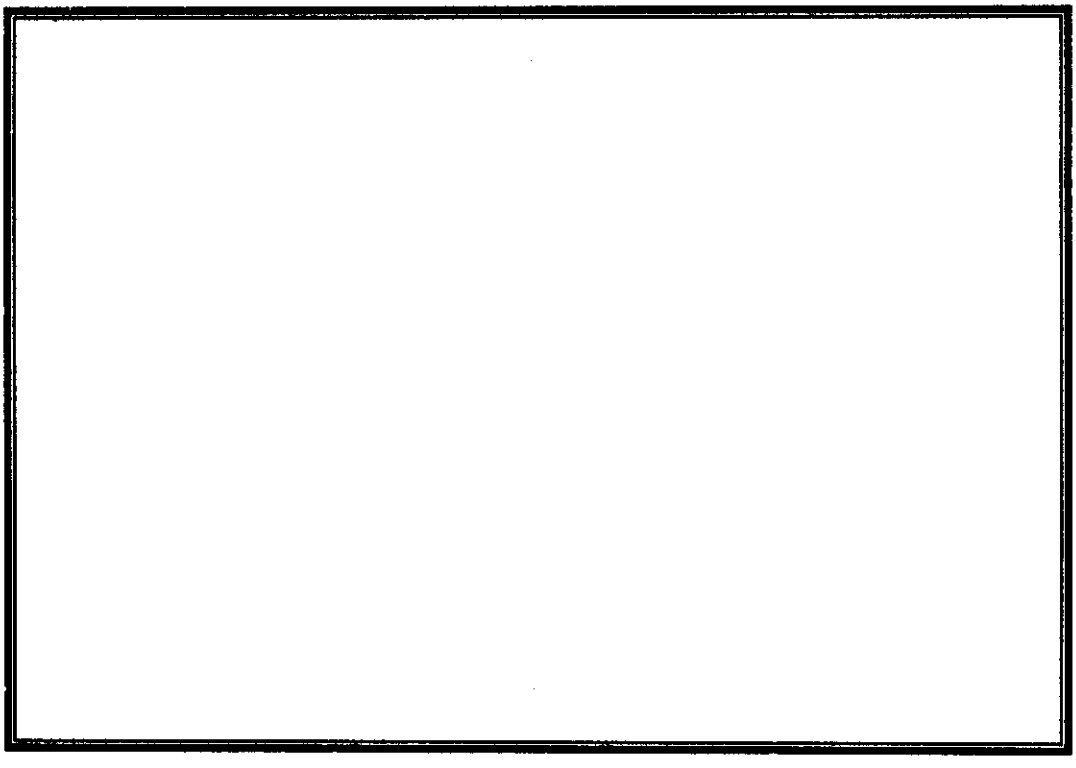

Fig. (38): Invasive duct carcinoma- breast showing positive p21 expression as a control (Streptavidin-Biotin x200).

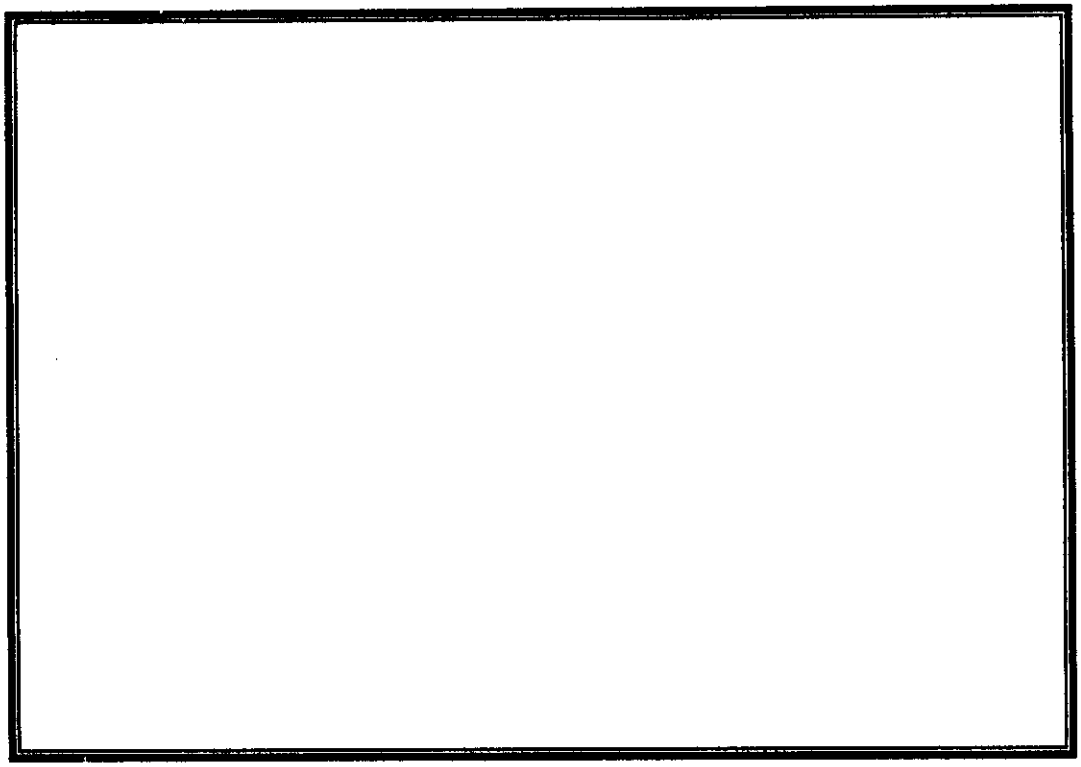

Fig. (39): Low-grade prostatic adenocarcinoma (G.S.S. 6, G2) showing positive nuclear p21 immunoreactivity (Streptavidin-Biotin x200).

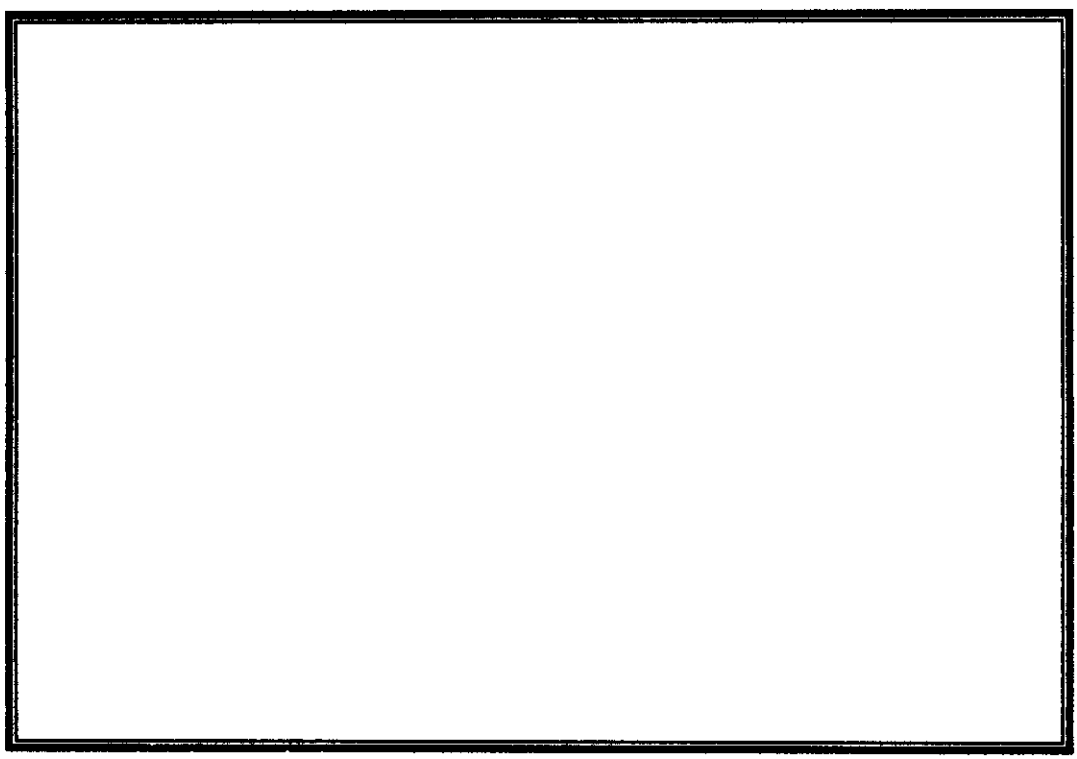

Fig. (40): Low-grade prostatic adenocarcinoma (G.S.S. 6, G2) showing positive nuclear p21 immunoreactivity (Streptavidin-Biotin x200).

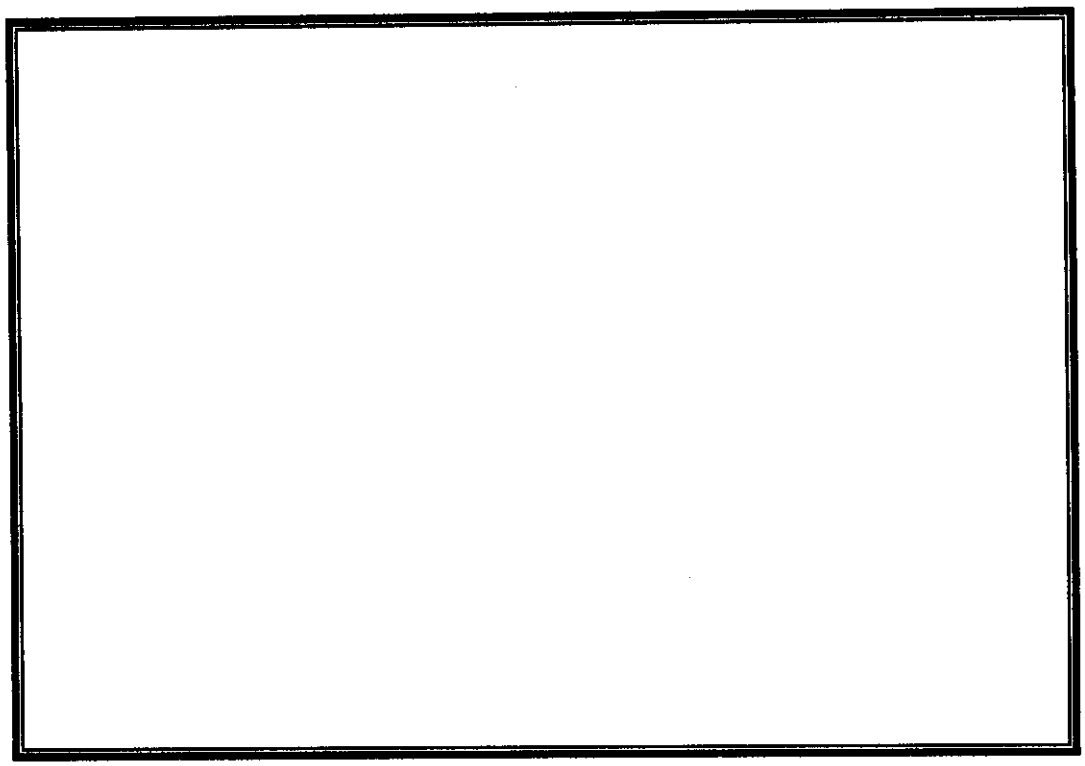

Fig. (41): High-grade prostatic adenocarcinoma (G.S.S. 7, G2) showing negative p21 immunoreactivity (Streptavidin-Biotin x200).